Utilizing Multi-Omics Analysis to Elucidate the Molecular Mechanisms of Oat Responses to Drought Stress

Xiaojing Chen , Jinghui Liu , Baoping Zhao , Junzhen Mi , Zhongshan Xu *

Posted Date: 20 January 2025

doi: 10.20944/preprints202501.1406.v1

Keywords: oat; drought stress; transcriptomics; proteomics; multi-omics

Article

Utilizing Multi-Omics Analysis to Elucidate the Molecular Mechanisms of Oat Responses to Drought Stress

Xiaojing Chen [1,2,3], Jinghui Liu [1,2], Baoping Zhao [1,2], Junzhen Mi [1,2] and Zhongshan Xu [1,2,*]

[1] National outstanding talents in agricultural research and their innovative teams, Hohhot, Inner Mongolia 010019, China

[2] Cereal Engineering Technology Research Center, Inner Mongolia Autonomous Region, Hohhot, Inner Mongolia, 010019, China

[3] College of Life Sciences,Inner Mongolia Agricultural University ,Hohhot, Inner Mongolia, 010019, China

* Correspondence: xzs1992@imau.edu.cn

Abstract: Oat is a crop and forage species with rich nutritional value, capable of adapting to various harsh growing environments, including dry and poor soils. It plays an important role in agricultural production and sustainable development. However, the molecular mechanisms underlying the response of oat to drought stress remain unclear, warranting further research. In this study, we conducted a pot experiment with drought-resistant cultivar JiaYan 2 (JIA2) and water-sensitive cultivar BaYou 9 (BA9) during the booting stage under three water gradient treatments: 30% field capacity (severe stress), 45% field capacity (moderate stress) and 70% field capacity (normal water supply). After 7 days of stress, root samples were collected for transcriptome and proteome analyses. Transcriptome analysis revealed that under moderate stress, JIA2 upregulated 1086 differential genes and downregulated 2919 differential genes, while under severe stress, it upregulated 1792 differential genes and downregulated 4729 differential genes. Under moderate stress, BA9 exhibited an upregulation of 395 differential genes, a downregulation of 669, and an upregulation of 886 differential genes and 439 downregulations under severe stress. In drought stress, most of the differentially expressed genes (DEGs) specific to JIA2 were downregulated, mainly involving redox reactions, carbohydrate metabolism, plant hormone signal regulation, and secondary metabolism. Proteomic analysis revealed that under moderate stress, 489 differential proteins were upregulated, and 394 were downregulated. Under severe stress, 493 differential proteins were upregulated, and 701 were downregulated. In BA9, 590 and 397 differential proteins were upregulated under moderate stress, with 126 and 75 upregulated differential proteins under severe stress. Correlation analysis between transcriptomics and proteomics demonstrated that compared with CK, four types of differentially expressed proteins (DEPs) were identified in the JIA2 differential gene-protein interaction network analysis under severe stress. These included 13 key cor DEGs and DEPs related to plant hormone signal transduction, biosynthesis of secondary metabolites, carbohydrate metabolism processes, and metabolic pathways. The consistency of gene and protein expression was validated using qRT-PCR, indicating their key role in the strong drought resistance of JIA2.

Keywords: oat; drought stress; transcriptomics; proteomics; multi-omics

1. Introduction

Under natural conditions, plant growth is often influenced by abiotic stresses such as drought, salinity, high temperatures, and cold. Enhancing crop stress resistance and developing new cultivars with improved tolerance and yield potential is currently the most economical strategy to boost agricultural productivity. Among these stresses, drought is one of the most detrimental

 doi:10.20944/preprints202501.1406.v1

environmental factors affecting plant growth and development. With the escalating impacts of global climate change, drought has become a global challenge that restricts plant productivity [1–3].

The inhibition of growth and development is one of the most evident plant responses to drought stress. Drought can result in reduced plant height, fewer nodes, decreased leaf area, lower dry matter accumulation, prolonged growth periods, and significantly reduced yields[4–6]. In response to drought, plants accumulate substantial amounts of organic compounds and inorganic ions to increase cell fluid concentration, lower osmotic potential, enhance water retention, maintain cellular structure and the spatial arrangement of biomacromolecules, and promote root growth under severe water-deficient conditions[7,8].

Proteomics and transcriptomics are extensively used to investigate plant responses to salt and drought stresses[9,10]. For example, studies have revealed that ribosomal genes, including RPL5, 10, 23, and 38, are abundant in alpha-linolenic acid metabolism in wheat grains under non-drought conditions. Key genes regulating wheat quality are significantly upregulated in alanine, aspartate, glutamate, nitrogen, and alpha-linolenic acid metabolisms[11]. Under drought stress, plant cells sense and process stress signals through signal sensors, converting extracellular signals into intracellular signals. These signals are transmitted through distinct transduction pathways, where plant hormones, second messengers, signal transducers, and transcriptional regulators play important roles[12]. Transcription factor families such as WRKY, NAC, bZIP, AP2/EREBP, and MYB are closely associated with gene expression regulation under water deficit conditions[13].

Oat (*Avena sativa* L.) is classified as a whole grain, rich in nutrients such as beta-glucan, fat, protein, minerals, and polyphenols[14]. As a dual-purpose crop for grain and feed, it exhibits drought and barrenness tolerance, making it well-suited for cultivation in arid and semi-arid regions. As an advantageous characteristic crop in Inner Mongolia, its planting area and total yield rank first in China, playing a significant role in the development of local agriculture and animal husbandry[15]. Drought inhibits oat growth, leading to reductions in plant height, dry matter accumulation rate, root length, area, and volume compared to conditions with adequate water supply[16]. To cope with drought, plants accumulate various organic or inorganic substances within cells to maintain the osmotic balance between intracellular and extracellular environments[17]. However, drought stress can increase osmotic pressure in oat cells, disrupting normal growth. Additionally, it lowers the net photosynthetic rate, transpiration rate, and stomatal conductance in oat leaves. Intercellular CO_2 concentration decreases under mild drought stress but increases under moderate and severe drought stress. During the critical period of drought stress, light, moderate, and severe drought led to yield reduction of 9.5% to 12.7%, 16.8% to 27.0%, and 44.1% to 47.7%, respectively[18]. Under drought stress, auxin, cytokinin, and brassinosteroid signaling pathways in Longyan 3 are inhibited, while abscisic and jasmonic acid signaling pathways are activated. Upregulation of genes such as PP2C, ABF, SNRK2, GID1, JAZ, and MYC2 may enhance drought resistance in DA92-2F6[19].

Currently, research on oat responses to drought stress primarily focuses on growth, physiological and biochemical indicators, and single omics studies (transcriptomics, proteomics, or metabolomics). Multi-omics association analysis has been applied to investigate oat responses to salt or phosphorus stress. However, no studies have used multi-omics association analysis to explore the drought resistance mechanism in oat[20]. Therefore, building on previous research from our group, this study selected oat cultivars with varying drought resistance and employed a combination of transcriptomics and proteomics to identify differentially expressed genes (DEGs) linked to drought resistance. Besides, we aimed to explore key metabolic pathways involved in oat responses to drought stress, providing a theoretical foundation and technical reference for breeding drought-resistant oat germplasm and advancing high-yield cultivation technology research.

 doi:10.20944/preprints202501.1406.v1

2. Results

2.1. Effects of Drought Stress on Growth Between Two Oat Cultivars

The growth of both cultivars was negatively affected by drought stress during the seedling stage. Under drought stress BA9 exhibited greater growth inhibition compared with JIA2, with BA9-1 demonstrating significantly better growth than BA9-2 and BA9-3 (Figure 1).

Figure 1. Growth comparison of two oat cultivars after drought stress. BA9-1, BA9-2, BA9-3, JIA2-1, JIA2-2, and JIA2-3 represent the normal water supply (70%) and moderate drought stress (45%) of BA9 and JIA 2 respectively) And severe drought stress (30%).

2.2. Transcriptome Sequencing Data Quality Control and Transcriptome Analysis

By assembling the complete BUSCO gene RNA-Seq reads from scratch, the mapping rate reached 88.75% (Figure 2A). Differential expression analysis of inter-sample data was performed using FPKM (Figure 2B), with a high correlation observed between the biological replicates of each treatment (Figure 2C). Based on these data, we can infer that the biological replicates of the sequencing samples are reliable, and a significant difference exists between drought stress and CK (Figure 2D).

 doi:10.20944/preprints202501.1406.v1

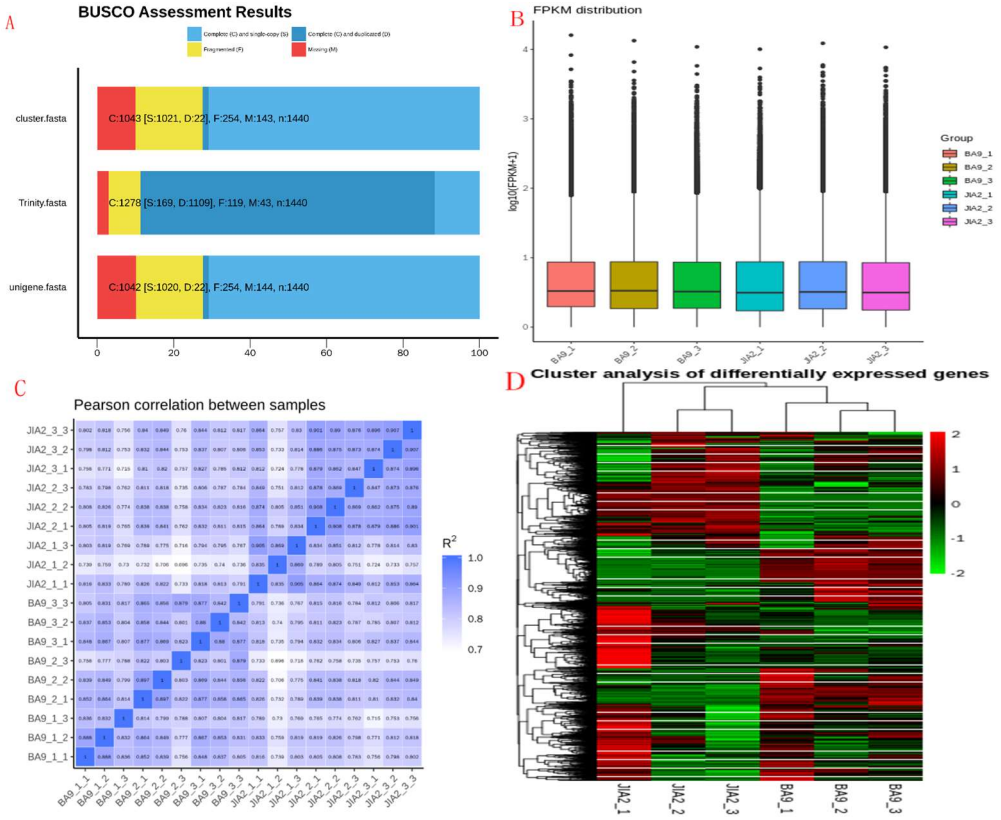

Figure 2. Sequencing sample evaluation.

This sequencing generated a total of 393,328 samples, with a total length of 566,345,053 bp. The longest sample was 13,283 bp, with an average length of 1,440 bp (Figure 3A). Sequence length analysis of the 393,328 transcripts revealed that 76.75% (301,870) of the sequences were below 2,000 bp. Specifically, there were 75,207 sequences under 500 bp, 105,908 between 500 and 1000 bp, 120,755 between 1,000 and 2,000 bp, and 91,458 sequences exceeding 2,000 bp (Figure 3B). Based on annotation results from the Nr library, species distribution maps on the comparison were statistically analyzed and plotted. The results indicated that the top species identified in the comparison were Boletus edulis, Aspergillus brevis, barley, wheat, Ural wheat, rice, and corn.

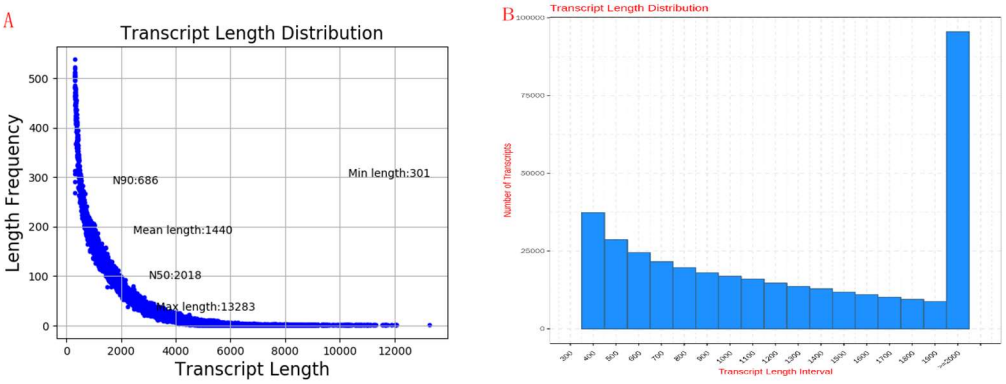

Figure 3. Transcript length distribution.

2.3. Annotations of Transcription Factors in Oat Roots with Different Drought Resistance Under Drought Stress

Under moderate stress, JIA2 differentially expressed transcription factors were classified into 10 categories, including 2 in MYB, 2 in WRKY, 1 in AP2, 1 in GATA, and 1 in HSF (Figure 4A). Under

 doi:10.20944/preprints202501.1406.v1

severe stress, JIA2 differentially expressed transcription factors were classified into 12 categories, including 3 in WRKY, 2 in MYB, 2 in HSF, 2 in bHLH, and 1 in GATA (Figure 4B).

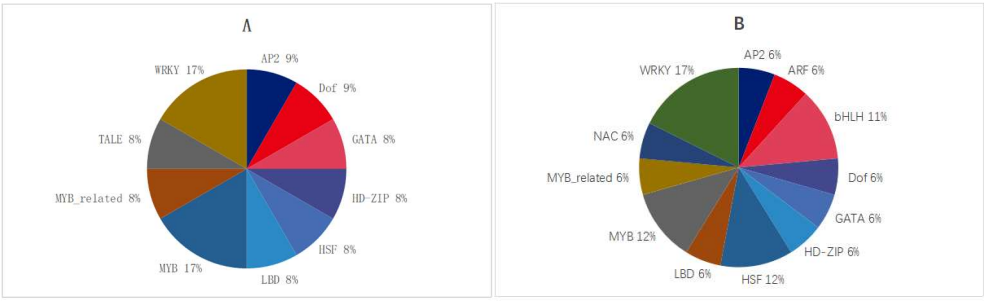

Figure 4. Differentially expressed transcription factors of JIA2 under drought stress. Note: A represents moderate drought stress treatment; B represents severe drought stress treatment.

Under moderate stress, no DEGs in BA9 were identified when compared with the Arabidopsis transcription factor database. Under moderate stress, three upregulated and nine downregulated DEGs in JIA2 were compared with the Arabidopsis transcription factor database (Table 1). Under severe stress, JIA2 exhibited 5 upregulated and 12 downregulated DEGs compared with the Arabidopsis transcription factor database (Table 2).

Table 1. Differentially expressed transcription factors of JIA2 under moderate drought stress.

Gene id	JIA2-1 FPKM	JIA2-2 FPKM	log2FC	qvalue	Family
Cluster-12329.30654	114.83	21.46	-2.53	0.000014	WRKY
Cluster-12329.9983	3.06	0.94	-1.81	0.008212	WRKY
Cluster-12329.32221	14.72	7.21	-1.14	0.005371	TALE
Cluster-12329.64361	10.23	2.90	-1.93	0.010695	MYB_related
Cluster-12329.56093	33.69	4.58	-2.99	0.000007	MYB
Cluster-12329.75409	16.84	0.58	-4.98	0.011413	MYB
Cluster-12329.25874	59.96	20.78	-1.65	0.000001	LBD
Cluster-12329.79361	4.14	0.95	-2.23	0.028308	HSF
Cluster-12329.54718	3.48	10.69	1.50	0.000001	HD-ZIP
Cluster-12329.44206	6.38	18.83	1.44	0.008599	GATA
Cluster-12329.33174	17.00	8.22	-1.16	0.000132	Dof
Cluster-12329.34327	3.62	9.08	1.21	0.014410	AP2

Table 2. Differentially expressed transcription factors of JIA2 under severe drought stress.

Gene id	JIA2-1 FPKM	JIA2-3 FPKM	log2FC	qvalue	Family
Cluster-12329.30654	114.83	4.11	-4.94	0.000001	WRKY
Cluster-12329.9983	3.06	0.97	-1.78	0.008281	WRKY
Cluster-12329.53056	34.44	10.04	-1.91	0.033821	WRKY
Cluster-12329.71925	7.99	1.75	-2.32	0.000012	NAC
Cluster-12329.64361	10.23	2.23	-2.33	0.000501	MYB_related
Cluster-12329.56093	33.69	1.14	-5.02	0.000001	MYB
Cluster-12329.75409	16.84	0.20	-6.55	0.006993	MYB
Cluster-12329.25874	59.96	13.16	-2.32	0.000001	LBD
Cluster-12329.79361	4.14	0.65	-2.80	0.003270	HSF
Cluster-12329.40676	2.91	12.27	1.95	0.005442	HSF
Cluster-12329.54718	3.48	12.03	1.66	0.000203	HD-ZIP

 doi:10.20944/preprints202501.1406.v1

Cluster-12329.44206	6.38	19.00	1.45	0.007739	GATA
Cluster-12329.33174	17.00	6.40	-1.54	0.000001	Dof
Cluster-12329.51794	1.08	5.33	2.16	0.006461	bHLH
Cluster-12329.49710	85.74	38.20	-1.30	0.024487	bHLH
Cluster-12329.54360	9.82	4.58	-1.23	0.008187	ARF
Cluster-12329.34327	3.62	9.86	1.31	0.000944	AP2

2.4. Identification of DEGs in Oats with Different Drought Resistance Under Drought Stress

Under moderate stress, BA9 identified 395 upregulated and 669 downregulated genes, while under severe stress, BA9 identified 886 upregulated and 439 downregulated genes. Under moderate stress, JIA2 identified 1,086 upregulated and 2,919 downregulated genes, while under severe stress, JIA2 identified 1,792 upregulated and 4,729 downregulated genes (Figure 5).

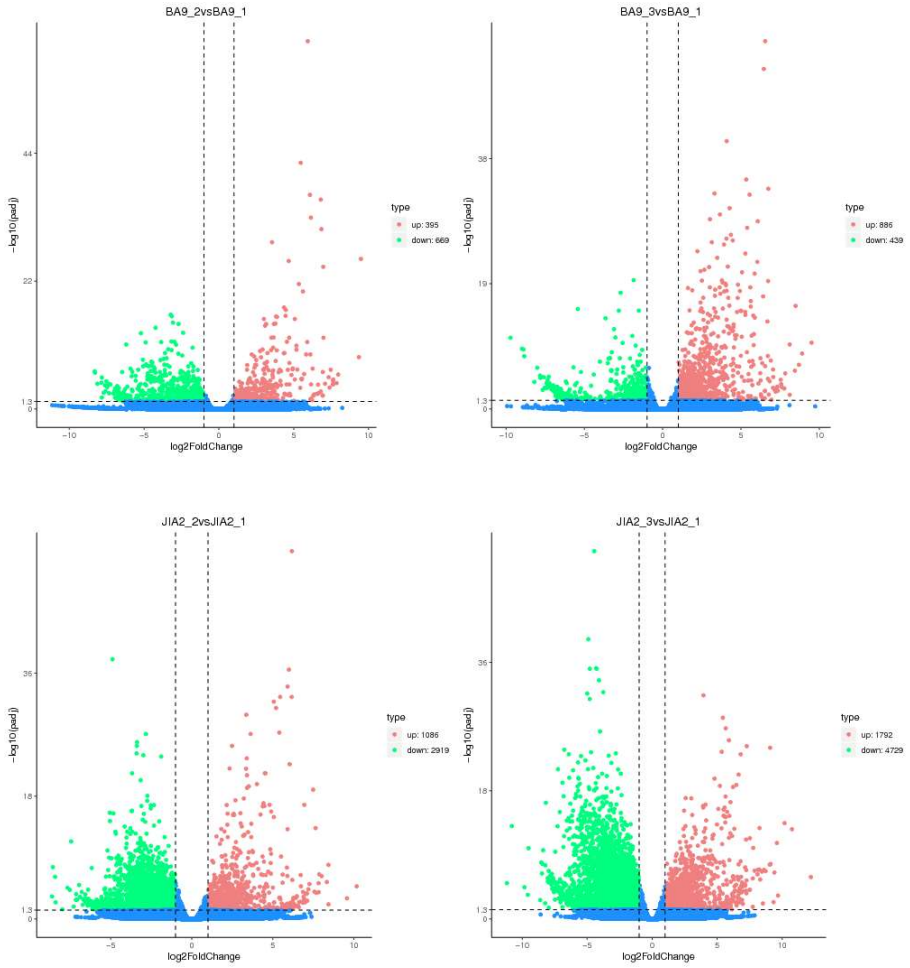

Figure 5. The number of differentially expressed genes in two oat cultivars under drought stress**.** Note: Red represents up-regulation, green represents down-regulation, and blue represents insignificant difference.

As presented in Table 3, the expression trends of the same DEGs under moderate and severe stress were consistent for BA9 and JIA2. Under the same stress conditions, the expression trend of the same genes in BA9 and JIA2 remained consistent. Table 4 lists the DEGs in JIA2 under drought stress. Under drought stress, the expression trend of the same genes was consistent, with most DEGs downregulated, mainly including redox reactions, carbohydrate metabolism, plant growth hormone signaling regulation, and secondary metabolism.

 doi:10.20944/preprints202501.1406.v1

Table 3. BA9 and JIA2 co-express differential genes under drought stress.

Gene id	log2FC/BA9-1		log2FC/JIA2-1		Description
	BA9-2	BA9-3	JIA2-2	JIA2-3	
Cluster-12329.57294	2.9	2.0	1.8	1.8	26 kDa endochitinase 1-like
Cluster-19271.0	-6.9	-5.9	-4.6	-7.0	40S ribosomal protein S6-B-like
Cluster-12329.5335	-7.5	-7.4	-4.3	-6.8	60S ribosomal protein L3
Cluster-25393.0	-4.7	-5.6	-3.7	-7.6	60S ribosomal protein L8-1-like
Cluster-12329.64025	4.1	5.2	5.9	9.1	ABA-inducible protein PHV A1-like
Cluster-12329.18166	5.2	5.8	4.6	7.3	ABA-inducible protein PHV A1-like
Cluster-12329.29340	-3.4	-5.2	-2.8	-4.7	actin 1
Cluster-12329.38263	-2.2	-1.6	-1.7	-1.5	alcohol dehydrogenase 3-like
Cluster-12329.7678	-5.2	-3.4	-7.4	-6.4	alpha-humulene synthase-like
Cluster-12329.42859	-1.9	-2.1	-1.5	-2.4	ammonium transporter AMT2.1
Cluster-12329.47412	2.0	1.3	1.0	1.5	AT-hook motif nuclear-localized protein 27-like
Cluster-12329.52341	-1.6	-1.4	-2.0	-2.2	bidirectional sugar transporter SWEET4
Cluster-12329.58240	1.5	1.3	2.8	3.4	bifunctional epoxide hydrolase 2-like
Cluster-12329.39029	1.3	1.9	1.2	2.9	CSC1-like protein HYP1
Cluster-12329.14410	1.7	1.8	1.3	1.4	dehydrin
Cluster-12329.43993	2.0	2.9	2.7	4.7	dehydrin-/LEA group 2-like protein
Cluster-12329.71405	2.5	3.0	1.5	2.3	delta-1-pyrroline-5-carboxylate synthase-like
Cluster-12329.58767	-1.4	-1.4	-2.5	-3.9	disease resistance protein RPM1 isoform X1
Cluster-12329.43994	2.8	3.9	4.5	6.7	drought acclimation dehydrin WZY2, partial
Cluster-12329.29658	-3.4	-5.3	1.7	-3.4	ervatamin-B-like isoform X1
Cluster-12329.40430	-2.3	-2.7	-3.7	-4.9	ethylene response factor
Cluster-12329.27606	3.2	4.5	3.0	4.3	eukaryotic peptide chain release factor subunit 1-2-like
Cluster-12329.32433	1.6	1.1	1.7	2.6	expansin-A11 isoform X1
Cluster-12329.42428	-3.7	-4.4	-3.0	-6.2	extensin-like
Cluster-12329.59588	1.5	1.6	1.1	2.6	G-box-binding factor 3 isoform X1
Cluster-12329.7992	-1.6	-1.2	-2.7	-3.8	G-type lectin S-receptor-like serine/threonine-protein kinase At1g34300
Cluster-12329.69532	3.0	3.6	2.1	3.9	Heat stress transcription factor C-2b
Cluster-12329.45966	-2.0	-1.9	-2.6	-4.0	heavy metal-associated isoprenylated plant protein 43-like
Cluster-12329.72154	2.3	3.8	2.4	3.8	hypothetical protein
Cluster-12329.58613	6.3	5.7	3.4	5.0	hypothetical protein BRADI_1g09260v3
Cluster-12329.6269	-2.8	-3.4	-2.1	-2.8	hypothetical protein BRADI_1g10635v3
Cluster-12329.47668	-1.7	-1.8	-1.9	-2.0	hypothetical protein BRADI_1g31700v3
Cluster-12329.16385	-1.4	-1.0	-3.0	-3.5	hypothetical protein BRADI_1g46170v3
Cluster-12329.16224	3.0	2.2	2.3	3.1	hypothetical protein BRADI_1g65230v3
Cluster-12329.6655	-2.3	-3.3	-4.6	-4.1	hypothetical protein BRADI_2g00467v3
Cluster-12329.71455	3.0	3.2	2.8	4.4	hypothetical protein BRADI_2g17200v3
Cluster-12329.14312	3.6	5.0	3.4	4.7	hypothetical protein BRADI_2g27180v3
Cluster-12329.10582	2.3	3.4	3.2	4.8	hypothetical protein BRADI_2g27810v3
Cluster-12329.48609	-1.8	-1.9	-1.4	-2.8	hypothetical protein BRADI_2g52970v3
Cluster-12329.76811	-1.9	-2.3	-2.1	-3.6	hypothetical protein BRADI_2g54660v3
Cluster-12329.60427	2.1	2.4	1.8	2.6	hypothetical protein BRADI_2g54920v3
Cluster-12329.16260	2.7	3.4	2.5	4.6	hypothetical protein BRADI_3g22635v3

 doi:10.20944/preprints202501.1406.v1

Cluster-12329.38859	-1.5	-2.8	-2.7	-3.9	hypothetical protein BRADI_4g02793v3
Cluster-12329.44891	-1.3	-1.3	-1.5	-2.3	hypothetical protein BRADI_4g31150v3
Cluster-12329.56429	-2.7	-2.2	-1.5	-2.6	hypothetical protein BRADI_5g03327v3
Cluster-12329.23994	2.2	2.1	2.8	4.0	hypothetical protein CUMW_252510, partial
Cluster-17139.0	-7.9	-7.8	-5.4	-5.4	hypothetical protein DD237_003955
Cluster-27360.1	-3.2	-6.5	-4.3	-5.2	hypothetical protein DYB32_000658
Cluster-12329.28366	-2.1	-1.2	-1.5	-2.5	hypothetical protein GQ55_2G049000
Cluster-12329.15541	2.5	2.8	1.9	3.0	hypothetical protein GQ55_5G192500
Cluster-12329.43996	3.6	4.5	4.0	6.2	hypothetical protein GQ55_8G157800
Cluster-12329.37837	4.4	5.3	5.5	7.5	hypothetical protein GQ55_9G600100
Cluster-12329.68880	2.1	2.7	2.8	4.1	hypothetical protein OsI_14820
Cluster-12329.57293	3.6	2.6	1.9	1.9	hypothetical protein OsJ_18467
Cluster-27955.0	-6.3	-7.2	-6.2	-6.2	hypothetical protein SELMODRAFT_419864
Cluster-12329.11108	4.1	4.5	2.8	4.1	hypothetical protein TRIUR3_02712
Cluster-12329.67466	2.9	3.1	2.5	3.9	hypothetical protein TRIUR3_04131
Cluster-12329.16582	6.1	5.9	3.3	5.4	hypothetical protein TRIUR3_14005
Cluster-12329.27476	-2.2	-1.6	-2.6	-3.5	hypothetical protein TRIUR3_18039
Cluster-12329.17145	6.8	6.4	4.9	7.3	hypothetical protein TRIUR3_24891
Cluster-12329.18011	2.5	2.3	3.1	3.7	jacalin-related lectin 19-like, partial
Cluster-12329.53964	2.8	4.0	4.4	6.7	late embryogenesis abundant protein 1
Cluster-12329.53965	3.4	4.3	4.5	6.8	late embryogenesis abundant protein, group 3-like
Cluster-12329.27453	4.4	5.1	3.1	5.6	late embryogenesis abundant protein, group 3-like
Cluster-12329.70282	5.6	5.8	5.5	7.9	late embryogenesis abundant protein, group 3-like
Cluster-12329.54680	3.2	3.0	2.8	3.7	linoleate 9S-lipoxygenase 2-like
Cluster-12329.30862	-1.5	-2.3	-2.8	-4.3	NAC domain-containing protein 21/22-like
Cluster-12329.59605	1.7	2.0	2.2	4.0	NADP-dependent malic enzyme
Cluster-12329.52489	-3.2	-2.8	-1.3	-2.0	nucleolar protein 58-like
Cluster-12329.73520	3.5	3.0	1.4	3.3	oleosin 1-like
Cluster-12329.59601	-3.2	-2.3	-3.3	-5.9	Peroxidase 15
Cluster-12329.33694	2.8	4.3	1.4	2.9	phytoene synthase 2, chloroplastic-like
Cluster-12329.15714	3.2	4.1	4.6	6.9	plasma membrane associated protein-1
Cluster-12329.73210	3.0	2.9	1.9	3.9	potassium channel KOR1-like isoform X1
Cluster-12329.82383	3.6	4.0	4.2	6.7	predicted protein
Cluster-30628.0	-6.6	-6.6	-3.5	-6.2	predicted protein
Cluster-12329.28775	3.8	3.2	2.0	3.5	predicted protein
Cluster-12329.12011	4.6	5.3	2.4	5.0	predicted protein
Cluster-12329.69415	5.2	3.5	1.8	2.5	predicted protein
Cluster-12329.38069	-1.3	-1.6	-1.3	-2.0	predicted protein
Cluster-12329.40903	-2.6	-2.2	-3.8	-4.6	predicted protein
Cluster-12329.5387	-2.5	-2.0	-2.9	-4.5	predicted protein
Cluster-12329.74926	4.9	4.5	2.9	3.9	predicted protein
Cluster-12329.69554	3.6	3.5	4.9	6.8	predicted protein
Cluster-12329.68697	5.9	6.1	5.1	7.8	predicted protein
Cluster-12329.15409	4.1	4.0	4.2	6.1	predicted protein
Cluster-12329.13801	4.3	6.5	4.7	8.1	predicted protein
Cluster-12329.60164	-2.5	-2.3	-1.5	-3.0	predicted protein
Cluster-12329.19357	2.4	2.8	1.8	2.8	predicted protein

 doi:10.20944/preprints202501.1406.v1

Cluster-12329.77573	-8.1	-5.2	-3.2	-5.4	predicted protein
Cluster-12329.29960	2.1	2.0	1.4	2.4	predicted protein
Cluster-12329.19255	3.9	3.9	3.7	5.6	predicted protein
Cluster-12329.14664	3.4	5.0	2.1	4.8	predicted protein
Cluster-12329.31089	3.2	2.4	1.9	2.2	predicted protein, partial
Cluster-12329.59227	-1.4	-1.1	-2.6	-3.5	probable calcium-transporting ATPase 6, plasma membrane-type
Cluster-12329.12846	2.3	2.6	1.6	3.1	probable fucosyltransferase 8
Cluster-12329.39746	-2.1	-1.6	-1.9	-2.5	probable LRR receptor-like serine/threonine-protein kinase At1g56140
Cluster-12329.50890	-1.5	-1.2	-1.7	-2.5	probable LRR receptor-like serine/threonine-protein kinase At1g56140
Cluster-12329.72876	-1.6	-1.7	-2.3	-2.9	probable LRR receptor-like serine/threonine-protein kinase At3g47570 isoform X1
Cluster-12329.57952	2.8	3.5	1.4	2.8	probable protein phosphatase 2C 50
Cluster-12329.13918	2.5	3.0	2.5	4.1	probable protein phosphatase 2C 8
Cluster-12329.54528	1.9	2.3	1.9	2.2	probable sucrose-phosphate synthase 5
Cluster-12329.19483	4.7	5.5	4.5	7.0	Protein LE25
Cluster-12329.53849	2.0	1.3	2.2	3.0	protein RETICULATA-RELATED 5, chloroplastic-like
Cluster-12329.70665	3.5	4.8	1.9	3.9	putative clathrin assembly protein
Cluster-12329.53530	-1.2	-1.3	-1.3	-1.5	putative disease resistance protein RGA3
Cluster-12329.12147	4.1	4.5	4.0	4.6	Putative invertase inhibitor
Cluster-12329.26350	-2.1	-2.4	-1.8	-2.8	putative receptor-like protein kinase At4g00960 isoform X1
Cluster-12329.54104	-2.0	-2.1	-1.9	-3.8	PYL3
Cluster-12329.70108	2.5	2.8	2.3	3.3	pyruvate decarboxylase 1-like
Cluster-12329.19311	2.3	2.6	2.2	3.9	retrotransposon protein, putative, Ty3-gypsy subclass
Cluster-12329.19313	1.7	2.1	1.3	2.0	retrotransposon protein, putative, Ty3-gypsy subclass
Cluster-12329.39137	-1.6	-1.1	-1.2	-1.4	Rp1-like protein
Cluster-12329.25017	-2.3	-2.4	-2.5	-2.7	SnTox1 sensitivity protein
Cluster-12329.29018	3.1	3.7	3.1	4.7	sucrose synthase 4
Cluster-12329.29020	3.0	3.5	3.0	4.6	sucrose synthase 4
Cluster-12329.21992	2.8	3.1	1.3	2.4	TB2/DP1 protein
Cluster-12329.17299	5.1	6.0	4.1	7.2	translocator protein homolog
Cluster-12329.74266	4.1	6.7	2.9	5.8	uncharacterized protein LOC100828693
Cluster-12329.42771	2.4	2.8	1.4	3.0	uncharacterized protein LOC100837178
Cluster-12329.43214	-1.5	-2.1	-2.8	-3.3	uncharacterized protein LOC104584952
Cluster-12329.48150	3.8	3.1	4.4	5.6	uncharacterized protein LOC109716535 isoform X1
Cluster-12329.17539	4.7	5.8	3.3	6.2	uncharacterized protein LOC109732782
Cluster-12329.83151	3.5	4.5	3.4	6.2	uncharacterized protein LOC109745464
Cluster-12329.69103	5.3	6.5	3.3	5.6	uncharacterized protein LOC109752199
Cluster-12329.70769	3.7	3.5	1.7	3.2	uncharacterized protein LOC109753512
Cluster-12329.18408	3.0	3.1	2.7	3.9	uncharacterized protein LOC109753512
Cluster-12329.19760	5.2	5.5	3.2	6.0	uncharacterized protein LOC109754768
Cluster-12329.30953	3.7	3.4	4.1	6.1	uncharacterized protein LOC109762444
Cluster-12329.14413	3.1	4.0	1.5	3.5	uncharacterized protein LOC109767342

 doi:10.20944/preprints202501.1406.v1

Cluster-12329.61249	1.9	1.9	1.3	2.0	uncharacterized protein LOC109772703
Cluster-12329.19134	4.5	5.3	3.2	5.5	uncharacterized protein LOC109773736
Cluster-12329.70583	6.1	6.6	3.8	6.3	uncharacterized protein LOC4331521
Cluster-19103.0	-6.2	-7.1	-5.7	-6.6	unknown
Cluster-12329.64076	-4.4	-6.8	-4.1	-5.1	unknown
Cluster-12329.27244	2.4	2.6	2.1	3.3	unnamed protein product
Cluster-12329.40591	3.1	2.3	2.1	2.9	unnamed protein product
Cluster-12329.65650	2.4	2.7	1.6	3.1	unnamed protein product
Cluster-12329.19319	4.3	4.2	3.6	5.7	unnamed protein product
Cluster-12329.20262	3.5	4.0	1.5	3.1	unnamed protein product
Cluster-12329.15018	-2.5	-2.1	-2.9	-5.6	unnamed protein product
Cluster-12329.69497	4.9	4.0	4.5	5.7	Vicilin-like antimicrobial peptides 2-2
Cluster-12329.10917	3.2	5.0	3.4	5.9	V-type proton ATPase subunit D-like
Cluster-12329.70389	2.4	3.2	2.6	2.5	wheatwin-2

Table 4. JIA2 specifically expresses differential genes under drought stress.

Gene id	JIA2-1 fpkm	JIA2-2 fpkm	JIA2-2 log2FC	JIA2-3 fpkm	JIA2-2 log2FC	Description
Cluster-12329.52838	9.9	649.1	5.9	549.6	5.7	--
Cluster-12329.76640	40.6	2.3	-4.2	1.8	-4.7	--
Cluster-12329.46046	3.2	154.3	5.5	395.2	6.8	--
Cluster-12329.52286	50.2	6.5	-3.1	6.3	-3.1	--
Cluster-12329.44964	250.5	33.8	-3.0	22.5	-3.6	1-aminocyclopropane-1-carboxylate oxidase-like
Cluster-12329.48023	176.2	23.4	-3.0	14.5	-3.7	1-aminocyclopropane-1-carboxylate oxidase-like
Cluster-12329.49732	392.4	48.5	-3.1	28.5	-3.9	ACC oxidase
Cluster-12329.49731	284.3	32.9	-3.2	19.2	-4.0	ACC oxidase
Cluster-12329.27503	30.4	2.6	-3.7	2.7	-3.6	aspartyl protease family protein At5g10770-like
Cluster-12329.55589	42.7	3.0	-4.0	2.6	-4.2	cysteine-rich receptor-like protein kinase 10
Cluster-12329.55590	31.3	3.7	-3.2	2.0	-4.1	cysteine-rich receptor-like protein kinase 10
Cluster-12329.22590	118.5	12.4	-3.4	4.7	-4.8	dirigent protein 5-like
Cluster-12329.40430	61.3	5.2	-3.7	2.2	-4.9	ethylene response factor
Cluster-12329.33234	60.6	7.4	-3.2	4.7	-3.8	glucan endo-1,3-beta-glucosidase 3-like isoform X1
Cluster-12329.33233	40.2	5.2	-3.1	3.7	-3.6	glucan endo-1,3-beta-glucosidase 3-like isoform X1
Cluster-12329.25273	64.7	7.9	-3.2	2.5	-4.8	heme-binding-like protein At3g10130, chloroplastic
Cluster-12329.8036	126.0	12.5	-3.4	2.6	-5.7	hypothetical protein BRADI_2g47510v3
Cluster-12329.56709	39.0	4.8	-3.1	3.4	-3.6	hypothetical protein BRADI_4g31430v3
Cluster-12329.74492	173.8	11.7	-4.0	7.0	-4.8	hypothetical protein OsI_20854
Cluster-12329.54760	104.1	11.9	-3.2	7.6	-3.9	hypothetical protein TRIUR3_01630
Cluster-12329.38808	32.3	4.1	-3.1	2.0	-4.2	hypothetical protein TRIUR3_31101
Cluster-12329.26155	151.9	17.8	-3.2	6.3	-4.7	IQ domain-containing protein IQM1
Cluster-12329.28038	40.9	461.8	3.4	683.5	3.9	metallothionein-like protein type 2
Cluster-12329.18219	150.5	16.1	-3.3	7.9	-4.4	mitogen-activated protein kinase kinase kinase 3-like
Cluster-12329.51406	152.6	19.1	-3.1	9.4	-4.2	phenylalanine ammonia-lyase 1
Cluster-12329.51405	134.3	15.4	-3.2	8.5	-4.1	phenylalanine ammonia-lyase 2
Cluster-12329.33610	60.7	7.3	-3.2	2.3	-4.9	predicted protein
Cluster-12329.77790	20.5	1.9	-3.5	2.2	-3.3	predicted protein

 doi:10.20944/preprints202501.1406.v1

Cluster-12329.10176	49.8	6.3	-3.1	4.3	-3.7	predicted protein
Cluster-12329.32862	167.9	20.2	-3.2	10.1	-4.2	predicted protein
Cluster-12329.40903	26.8	2.0	-3.8	1.2	-4.6	predicted protein
Cluster-12329.55591	23.7	2.4	-3.4	1.3	-4.3	predicted protein
Cluster-12329.62594	4.4	90.1	4.2	192.6	5.3	predicted protein
Cluster-12329.51932	162.6	13.2	-3.8	18.7	-3.3	predicted protein
Cluster-12329.68011	79.4	4.2	-4.3	2.8	-5.0	predicted protein, partial
Cluster-12329.24188	217.1	27.7	-3.1	2.8	-6.4	predicted protein, partial
Cluster-12329.46439	196.6	26.2	-3.0	18.9	-3.5	PREDICTED: cationic peroxidase SPC4-like
Cluster-12329.65038	54.8	7.2	-3.1	4.4	-3.8	probable calcium-binding protein CML10
Cluster-12329.54015	84.5	6.6	-3.8	5.5	-4.1	probable carboxylesterase 15
Cluster-12329.54017	70.2	6.8	-3.5	4.6	-4.1	probable carboxylesterase 15
Cluster-12329.53604	131.3	11.6	-3.6	5.4	-4.7	probable WRKY transcription factor 70
Cluster-12329.66018	396.5	40.6	-3.4	19.2	-4.5	protein TIFY 11e-like
Cluster-12329.66019	182.6	19.7	-3.3	8.5	-4.6	protein TIFY 11e-like
Cluster-12329.53548	57.4	7.4	-3.1	6.9	-3.2	putative acyl transferase 6
Cluster-12329.55264	69.5	9.3	-3.0	2.0	-5.2	Putative disease resistance RPP13-like protein 1
Cluster-12329.24192	88.8	11.9	-3.0	2.1	-5.6	putative WRKY transcription factor 46
Cluster-12329.44119	93.5	12.3	-3.0	12.6	-3.0	Q-type C2H2 zinc finger protein
Cluster-12329.23063	81.4	8.8	-3.3	3.1	-4.9	RING-H2 finger protein ATL3-like
Cluster-12329.23854	45.4	5.1	-3.3	3.1	-4.0	serine/threonine-protein kinase RIPK
Cluster-12329.30337	31.3	4.1	-3.0	1.8	-4.2	U-box domain-containing protein 27
Cluster-12329.10245	35.3	1.7	-4.5	1.7	-4.5	uncharacterized protein LOC109741409
Cluster-12329.7920	65.7	7.1	-3.3	5.6	-3.7	uncharacterized protein LOC109765335
Cluster-12329.7921	37.1	4.2	-3.3	1.5	-4.8	uncharacterized protein LOC109765335
Cluster-12329.23823	28.4	350.5	3.5	519.5	4.0	uncharacterized protein LOC109783551
Cluster-12329.40403	6.0	57.5	3.1	55.5	3.1	uncharacterized protein LOC109783551
Cluster-12329.9976	79.3	8.2	-3.4	2.3	-5.3	uncharacterized protein LOC109784088
Cluster-12329.32861	113.7	12.1	-3.3	4.6	-4.8	unnamed protein product
Cluster-12329.61828	18.7	2.1	-3.3	2.2	-3.2	unnamed protein product
Cluster-12329.39006	21.0	2.8	-3.0	1.7	-3.8	wall-associated receptor kinase 2-like

Note: The screening criteria for specifically expressed genes are $|\log2FC|>3$, $p<0.05$.

2.5. GO and KEGG Enrichment Analyses of DEGs

GO classification of DEGs indicated that, under moderate stress, BA9 genes were mainly enriched in response to stimuli (120), oxidoreductase activity (97), redox processes (88), and response to stress (88). Under severe stress, BA9 genes were mainly enriched in catalytic activity (458), oxidoreductase activity (132), redox processes (129), structural molecular activity (77), peptide metabolism processes (70), and ribosomes (67). For JIA2, under moderate stress, DEGs were mainly enriched in metabolic processes (1,569), catalytic activity (1,476), organic metabolism processes (1,315), and primary metabolism processes (1,252). Under severe stress, JIA2 genes were mainly enriched in metabolic processes (2,460), catalytic activity (2,352), ion binding (1,475), and transferase activity (1,085). The results indicate that biological metabolic processes and molecular functions represent the most significant responses to drought stress in both oat cultivars. Furthermore, under drought stress, BA9 exhibited the most pronounced changes in redox activity and process, while JIA2 demonstrated the most significant changes in metabolic processes (Figure 6).

 doi:10.20944/preprints202501.1406.v1

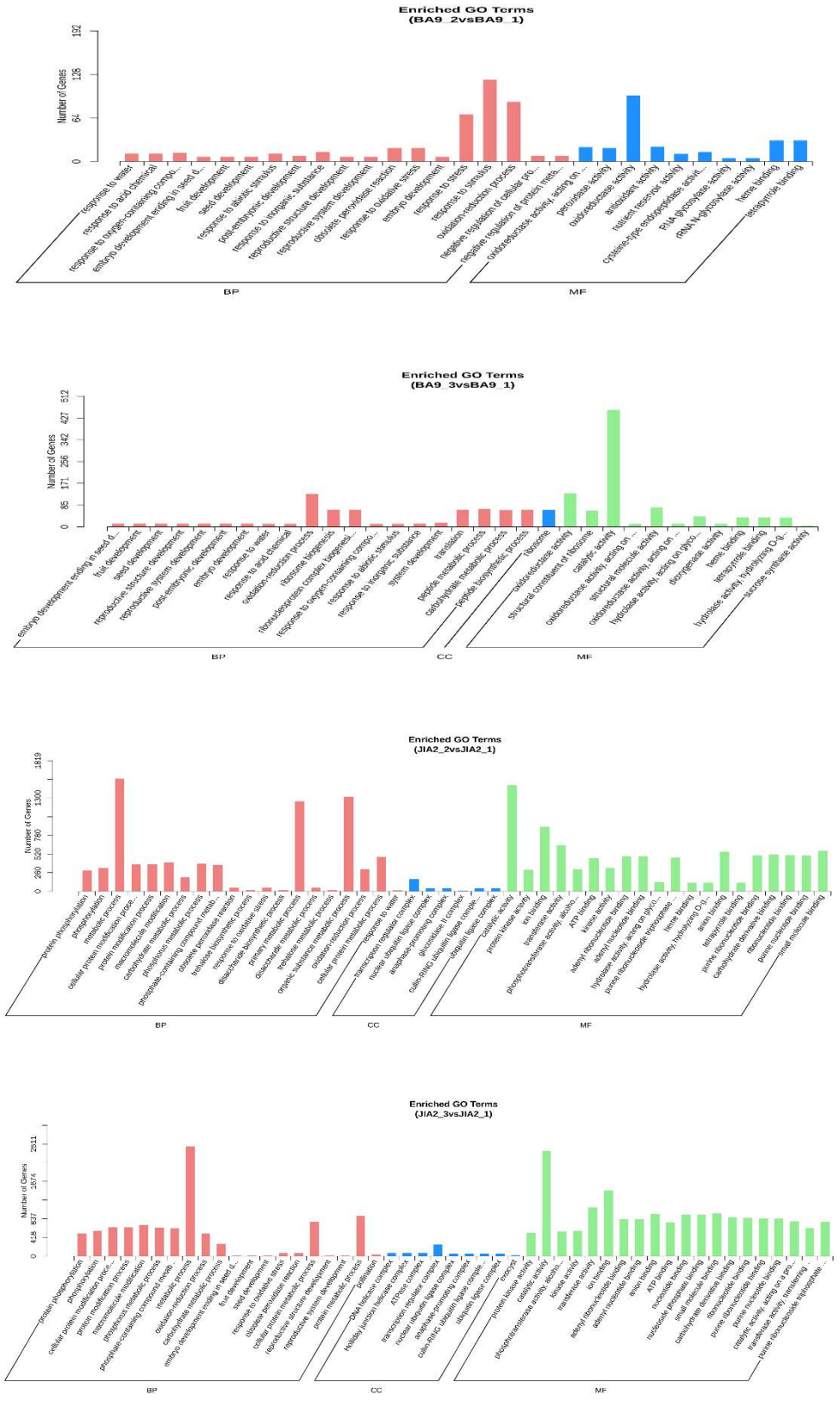

Figure 6. Analysis of GO Enrichment of Differentially Expressed Genes in Oat under Drought Stress.

The KEGG database was used to identify the primary metabolic pathways associated with DEGs. Under moderate stress, the co-upregulated genes in BA9 and JIA2 were predominantly involved in starch and sucrose metabolism (6/30; numbers represent the genes in the BA9/JIA2 pathways, respectively), phenylpropane biosynthesis (4/22), galactose metabolism (5/8), carotenoid biosynthesis (1/3), and linoleic acid metabolism (4/3). Pathways uniquely upregulated in BA9 genes

 doi:10.20944/preprints202501.1406.v1

under moderate stress included plant hormone signal transduction (10), glycolysis (5), butyrate metabolism (2), pentose phosphate pathway (3), fructose and mannose metabolism (3), RNA degradation (4), pyruvate metabolism (3), arginine and proline metabolism (2). The most significant pathways uniquely upregulated in JIA2 genes under moderate stress included gene replication (12), cyanide amino acid metabolism (13), pyrimidine metabolism (10), homologous recombination (5), nitrogen metabolism (6), and purine metabolism (8). The co-downregulated genes in BA9 and JIA2 under moderate stress were mainly associated with phenylpropane biosynthesis (39/95; numbers represent the genes in BA9/JIA2, respectively), phenylalanine metabolism (17/29), biosynthesis of phenylalanine, tyrosine, and tryptophan (3/7), and cyanide amino acid metabolism (4/20). The most significant pathways uniquely downregulated in BA9 genes under moderate stress included ribosomes (41), whereas, in JIA2, they involved starch and sucrose metabolism (50), plant-pathogen interactions (47), linoleic acid metabolism (10), plant hormone signal transduction (30), galactose metabolism (13), and flavonoid biosynthesis (11).

The metabolic pathways involved in the co-upregulation of BA9 and JIA2 genes under severe stress were mainly concentrated in carotenoid biosynthesis (10/5; numbers represent genes in BA9/JIA2, respectively), plant hormone signal transduction (19/17), glycolysis (16/19), galactose metabolism (9/18), protein processing in the endoplasmic reticulum (20/28), linoleic acid metabolism (5/5), starch and sucrose metabolism (14/43), arginine and proline metabolism (6/11), butyrate metabolism (3/3), carbon fixation in photosynthetic organisms (5/10), and pyruvate metabolism (5/16). The most significant pathways uniquely upregulated in BA9 genes under severe stress included lipid metabolism (9), endocytosis (14), spliceosome (13), pentose phosphate pathway (5), and β-alanine metabolism (4). In contrast, the pathways uniquely upregulated in JIA2 genes under severe stress included cyanide amino acid metabolism (18), DNA replication (11), homologous recombination (11), phenylpropane biosynthesis (33), fructose and mannose metabolism (10), alanine, aspartate, and glutamate metabolism (10), and RNA degradation (12). The metabolic pathways involved in the co-downregulation of BA9 and JIA2 genes under severe stress were mainly concentrated in phenylpropanoid biosynthesis (15/124), ubiquinone and other terpenoid quinone biosynthesis (2/16), alpha-linolenic acid metabolism (2/15), and tyrosine metabolism (3/10). The most significant pathways uniquely downregulated in BA9 genes under severe stress included ribosome (61) and the metabolism of cysteine and methionine (7). In contrast, pathways uniquely downregulated in JIA2 genes involved plant-pathogen interaction (83), phenylalanine metabolism (39), flavonoid biosynthesis (32), linoleic acid metabolism (14), plant hormone signal transduction (45), starch and sucrose metabolism (49), glutathione metabolism (29), circadian rhythm in plants (12), and biosynthesis of phenylalanine, tyrosine, and tryptophan (12).

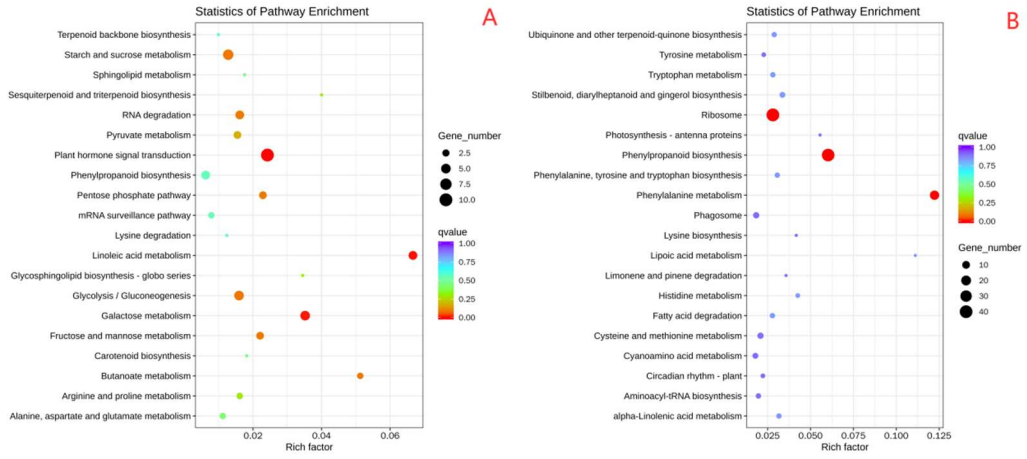

 doi:10.20944/preprints202501.1406.v1

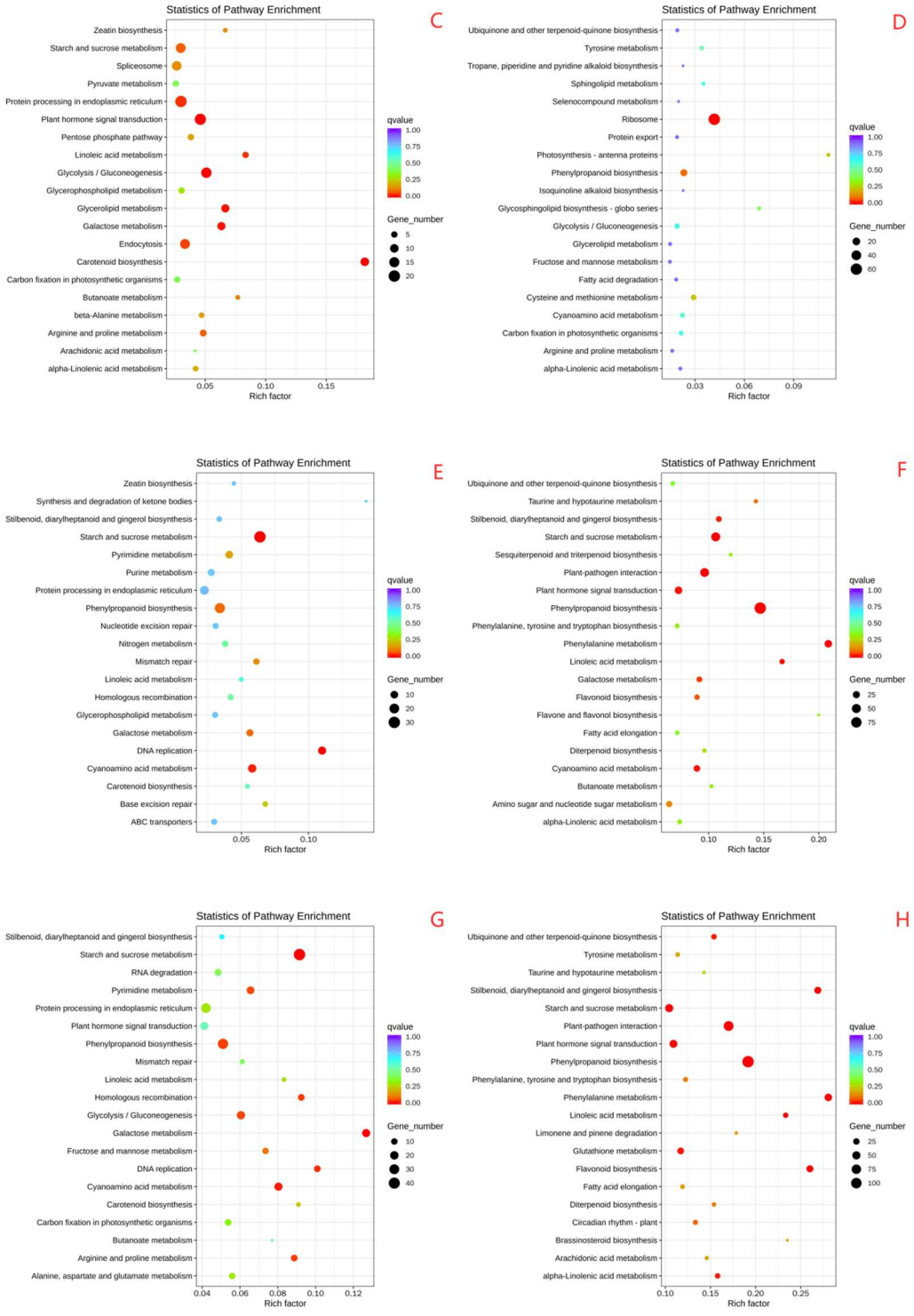

Figure 7. Analysis of KEGG Enrichment of Differentially Expressed Genes in Oats under Drought Stress**.** Note: A represents BA9-2 treatment up-regulated genes; B represents BA9-2 treatment down-regulated genes; C represents BA9-3 treatment up-regulated genes; D represents BA9-3 treatment down-regulated genes; E represents JIA2-2 treatment up-regulated genes; F represents JIA2 -2 treatment down-regulated genes; G represents JIA2-3 treatment up-regulated genes; H represents JIA2-3 treatment down-regulated genes.

2.6. Effects of Drought Stress on the Transcriptomes in Oat Roots

To further explore oat gene resources, SSR, SNP, and InDel markers were identified in the two tested oat root samples. A total of 18,799 SSR markers were detected. Statistical analysis revealed that single nucleotide repeat types were the most prevalent, comprising 6,996 (37.21%), followed by

 doi:10.20944/preprints202501.1406.v1

trinucleotide repeat types at 6,989 (37.18%), dinucleotide repeat types at 4,054 (21.56%), and other types accounting for 760 (4.05%). Among the SNP and InDel detection sites, 573,338 were substitution types, including 284,823 C/T types (49.68%) and 288,515 A/G types (50.32%). Additionally, 350,933 types of switching were identified, consisting of 62,301 A/T types (17.76%), 90,623 A/C types (25.82%), 89,980 T/G types (25.64%), and 108,029 C/G types (30.78%).

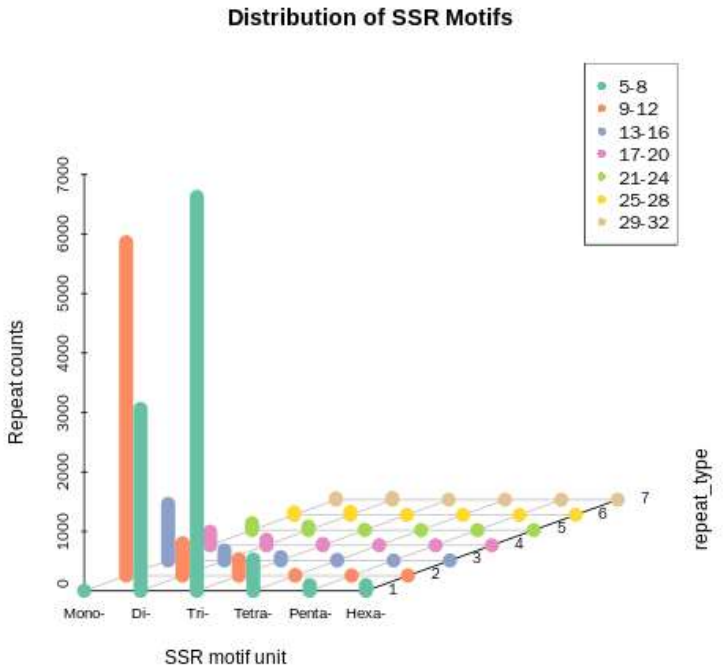

Figure 8. SSR statistics.

2.7. Protein Functional Annotation Analysis

GO functional annotation was performed on the root tissues of two oat cultivars across all treatments (Figure 9A). A total of 5,064 DEPs were annotated, involving 1,104 entries. The top 10 categories are as follows: biological processes: oxidation-reduction, metabolic and carbohydrate metabolic processes, translation, proteolysis, protein phosphorylation, response to oxidative stress, intracellular protein transport, transport, and transmembrane transport; cellular components: membrane, ribosome, integral component of membrane, intracellular, cytoplasmic, nucleus, nucleosome, extracellular region, proteasome core complex, and endoplasmic reticulum. Molecular functions: oxidoreductase, catalytic, and peroxidase activities; ATP, GTP, RNA, protein, heme, and nucleic acid bindings; and structural constant of the ribosome.

KEGG functional annotation was performed on oat root tissues from two cultivars across all treatments (Figure 9B), identifying a total of 8,093 DEPs. These proteins were categorized into five hierarchical categories and 19 metabolic pathways: cellular processes: transport and catabolism; environmental information processing: signal transduction and membrane transport; genetic information processing: transcription, translation, replication, and repair, and folding, sorting, and degradation; metabolism: nucleotide, lipid, cofactors and vitamins, energy, carbohydrate, terpenoids and polyketides, other amino acids, global and overview maps, glycan biosynthesis, and secondary metabolites biosynthesis; organic systems: environmental adaptation.

COG functional annotation was performed on oat root tissues from two cultivars across all treatments (Figure 9C), identifying 4,073 DEPs. The annotation results (Figure 9C) revealed the following numbers of proteins in each category: carbohydrate transport and metabolism (508), post-translational modification, protein turnover, and chaperones (505), translation, ribosomal structure

 doi:10.20944/preprints202501.1406.v1

and biogenesis (496), general function prediction only (479), amino acid transport and metabolism (338), energy production and conversion (312), lipid transport and metabolism (279), signal transduction mechanisms (258), secondary metabolites biosynthesis, transport and catabolism (227), coenzyme transport and metabolism (171), cell wall, membrane, and envelope biogenesis (169), inorganic ion transport and metabolism (129), nucleic acid transport and metabolism (128), defense mechanisms (125), translation and transcription (113), replication, recombination, and repair (106), cell cycle control, cell division, and chromosome partitioning (39), cytoskeleton (25), cell motility (18), intracellular transport, secretion, and vesicle transport, circular traffic, secrecy, and vascular transport (11) 1), chromatin structure and dynamics (9), extracellular structures (4), RNA processing and modification (3), mobile group: prophages, transposons (3), and function unknown (55).

IPR functional annotation was performed on oat root tissues from two cultivars across all treatments (Figure 9D), identifying 6,784 DEPs. The annotation results indicated the following numbers of proteins in each category: protein kinase domain (153), heme peroxidase [plant/fungal/bacterial (143)], plant peroxidase (126), RNA recognition motif domain (119), WD40 repeat (95), domains containing WD40 repeat sequences, WD40 peak containing domains (88), UDP-glucuronosyl/UDP-glucosyltransferase (85), cytochrome P450 (81), AAA + ATPase domain (76), glutathione-S-transferase [C-terminal like (55)], EF-hand domain (55), serine-threonine/tyrosine kinase catalytic domain (55), helicase superfamily 1/2 ATP binding domain (52), bifunctional inhibitor/plant lipid transfer protein/seed storage helical domain (52), small GTPase superfamily (49), glutathione S-transferase [N-terminal (49)], helicase C-terminal (47), heat shock protein 70 family (46), and ABC transporter-like (43).

The results of this study (Figure 9F) revealed 3,061 DEPs, categorized into 12 categories: cytoplasmic proteins (674, 20.02%), nuclear proteins (459, 15.00%), cell membrane proteins (404, 13.20%), mitochondrial proteins (370, 12.09%), chloroplast proteins (325, 10.62%), endoplasmic reticulum proteins (230, 7.51%), vacuolar proteins (162, 5.29%), peroxisome protein (120, 3.92%), and others.

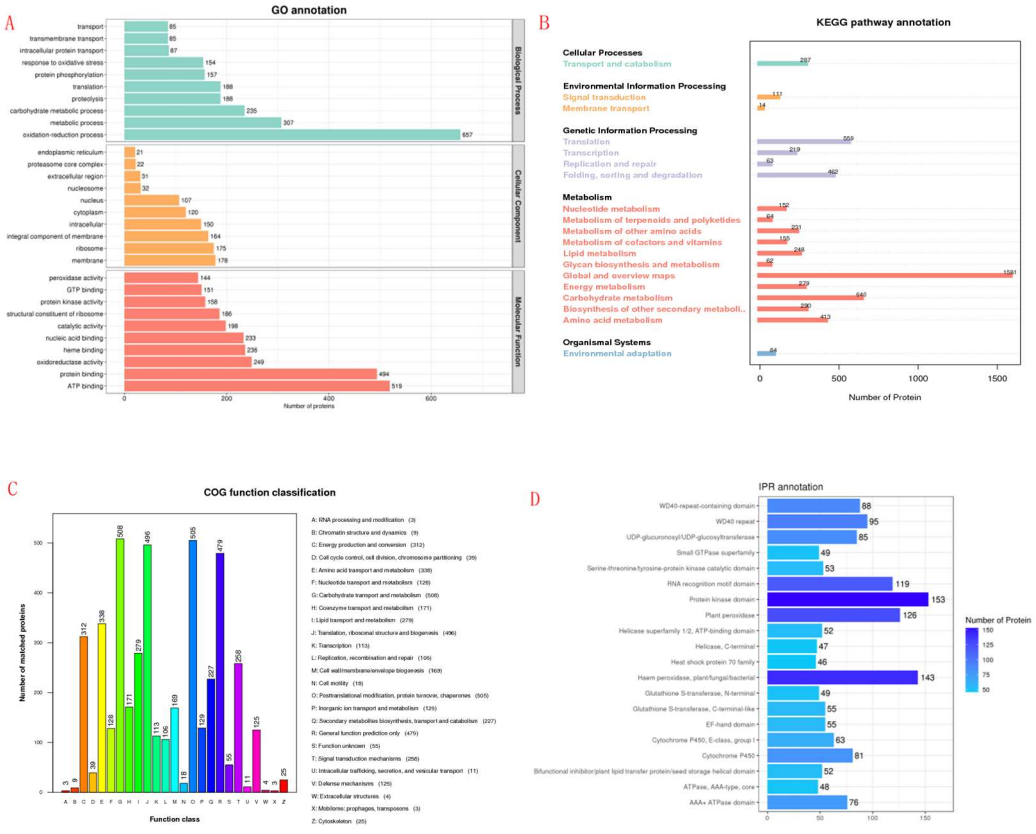

 doi:10.20944/preprints202501.1406.v1

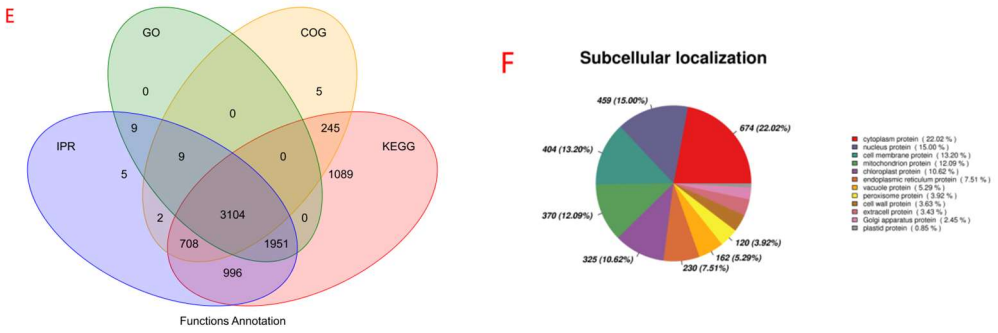

Figure 9. Function classification map**.** Note: A is the GO function classification diagram; B is the KEGG classification diagram; C is the COG function classification diagram; D is the IPR function annotation; E is the petal diagram of each database classification; F is the subcellular location diagram.

2.8. Identification of DEPs

As depicted in Figure 10, under moderate stress, BA9 exhibited 590 upregulated and 397 downregulated DEPs, while under severe stress, BA9 exhibited 126 upregulated and 75 downregulated proteins. Under moderate stress, JIA2 exhibited 489 upregulated and 394 downregulated DEPs, while under severe stress, JIA2 exhibited 493 upregulated and 701 downregulated proteins. Significant differences were observed in the number of upregulated and downregulated proteins between BA9 and JIA2 under severe stress (Figure 11).

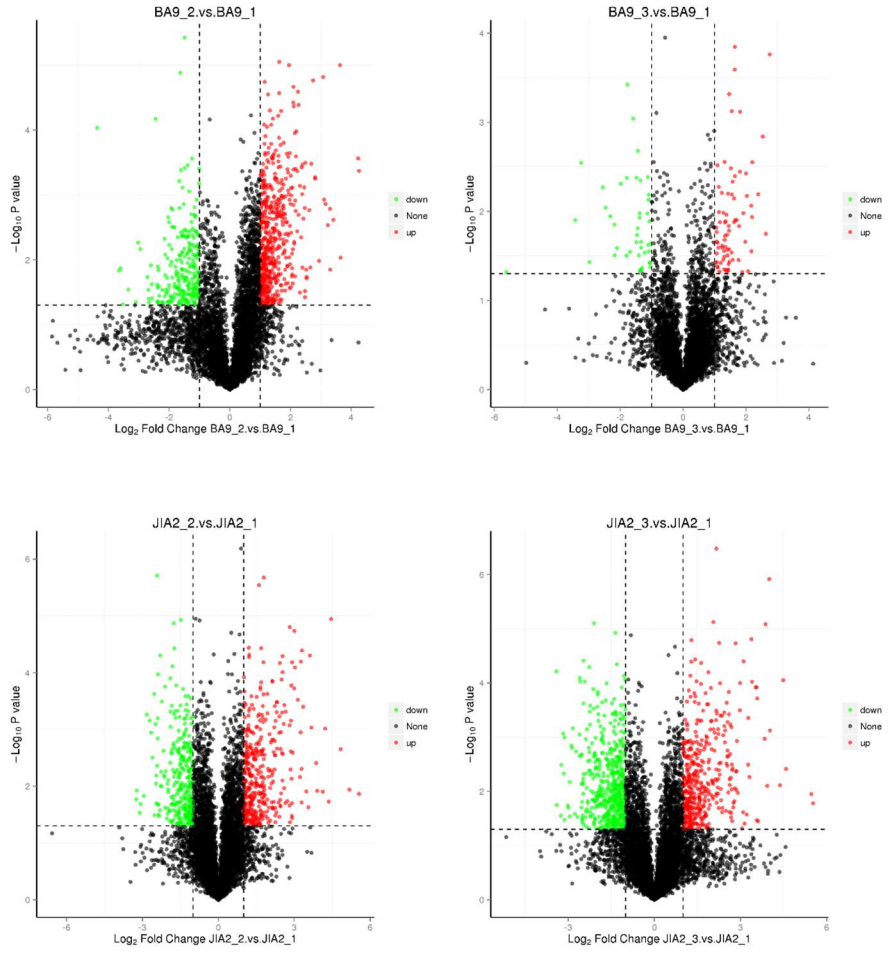

Figure 10. Volcano map of differentially expressed proteins of two cultivars under drought stress Note: Select when FC≥2.0 and Pvalue≤0.05 to screen for up-regulated expression proteins, when FC≤0.50 and Pvalue≤0.05, screen for down-regulated expression proteins.

 doi:10.20944/preprints202501.1406.v1

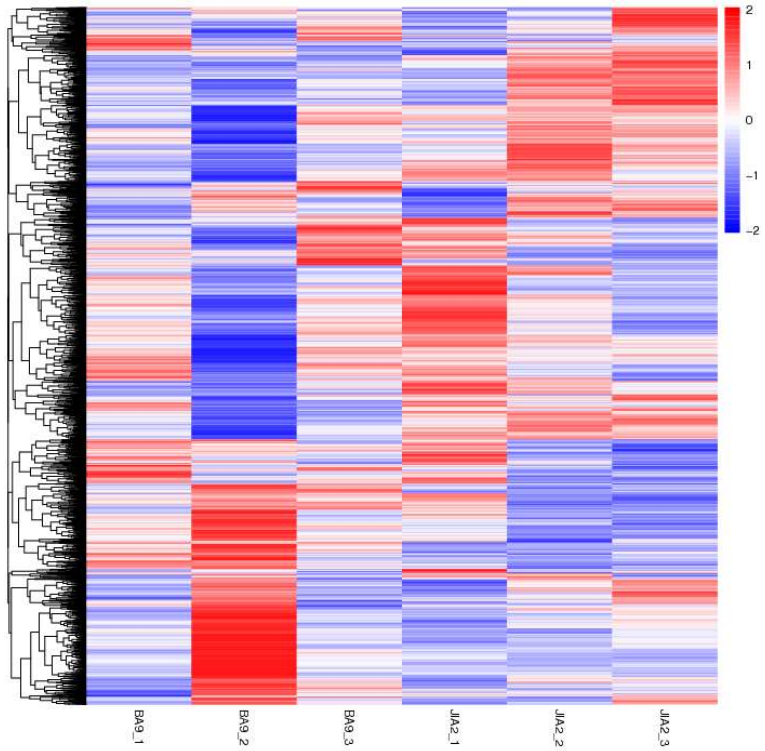

Figure 11. Cluster map of differentially expressed proteins of two cultivars under drought stress.

The DEPs co-expressed by BA9 and JIA2 under drought stress are listed in Table 7, with most displaying consistent expression trends between the two cultivars. Under drought stress, 314 specific DEPs were detected in JIA2. The number of upregulated and downregulated proteins was roughly equal, with functions primarily involving the structural constant of the ribosome, protein binding, oxidation-reduction process, metabolic process, integral membrane components, catalytic activity, carbohydrate metabolic process, and other functions.

Table 5. BA9 and JIA2 co-express differential proteins under drought stress.

Gene id	Description	BA9-2/9-1		BA9-3/9-1		JIA2-2/2-1		JIA2-3/2-1	
		FC	p-value	FC	p-value	FC	p-value	FC	p-value
Cluster-12329.42730	12-oxo-phytodienoic acid reductase 2	0.457	0.002	0.564	0.004	0.568	0.001	0.530	0.000
Cluster-12329.40415	26 kDa endochitinase 1-like	3.224	0.000	2.921	0.001	2.143	0.042	2.809	0.009
Cluster-12329.39510	ABC transporter G family member 48-like	2.081	0.002	1.828	0.020	0.985	0.973	1.140	0.781
Cluster-12329.30175	Adipocyte plasma membrane-associated protein	3.083	0.000	1.724	0.001	0.682	0.027	0.603	0.013
Cluster-12329.40387	alpha-galactosidase-like	0.656	0.017	1.556	0.024	1.160	0.742	1.468	0.305
Cluster-12329.42859	ammonium transporter AMT2.1	0.378	0.004	0.456	0.011	0.120	0.108	0.134	0.110

 doi:10.20944/preprints202501.1406.v1

Cluster-12329.58512	anthranilate synthase alpha 2 subunit	0.348	0.004	0.521	0.003	0.590	0.005	0.421	0.002
Cluster-12329.42873	ATP-citrate synthase alpha chain protein 2	3.520	0.002	2.604	0.011	1.428	0.448	1.520	0.449
Cluster-12329.25236	berberine bridge enzyme-like 27	0.356	0.000	0.555	0.007	0.310	0.001	0.282	0.001
Cluster-12329.46928	beta-glucosidase 4	1.761	0.011	2.979	0.035	1.433	0.303	1.829	0.238
Cluster-12329.48569	cinnamyl alcohol dehydrogenase	0.369	0.041	0.542	0.031	0.821	0.352	0.733	0.229
Cluster-12329.46789	cytochrome P450	0.548	0.047	0.674	0.024	0.566	0.051	0.612	0.075
Cluster-12329.48221	cytochrome P450	1.656	0.012	1.428	0.036	0.304	0.033	0.294	0.032
Cluster-12329.18884	cytochrome P450 CYP99A1-like	2.200	0.011	2.632	0.018	2.218	0.003	1.555	0.286
Cluster-12329.53808	cytosolic Cu/Zn superoxide dismutase	0.770	0.044	1.424	0.025	1.341	0.002	1.381	0.006
Cluster-12329.22699	dicarboxylate transporter 2.1, chloroplastic	0.611	0.038	0.627	0.028	1.170	0.544	1.766	0.220
Cluster-12329.47448	E3 ubiquitin-protein ligase KEG	2.610	0.001	3.691	0.048	1.191	0.158	0.971	0.872
Cluster-12329.38222	electron transfer flavoprotein-ubiquinone oxidoreductase, mitochondrial isoform X3	0.459	0.048	0.478	0.038	2.809	0.002	2.571	0.001
Cluster-12329.47209	elongation factor-like GTPase 1	1.791	0.040	1.483	0.040	1.080	0.569	1.416	0.119
Cluster-12329.43587	fructan exohydrolase	0.664	0.026	0.503	0.010	0.284	0.000	0.234	0.000
Cluster-12329.44239	hydroxyanthranilatehydroxycinnamoyltransferase 3	0.768	0.031	0.555	0.001	0.544	0.050	1.012	0.982
Cluster-12329.29762	hypothetical protein BRADI_1g07910v3	1.580	0.009	1.414	0.028	1.515	0.008	1.340	0.086
Cluster-12329.45583	hypothetical protein BRADI_2g08250v3	0.816	0.040	0.727	0.046	0.560	0.001	0.487	0.000
Cluster-12329.46014	hypothetical protein BRADI_2g42380v3	1.449	0.012	1.738	0.035	1.145	0.729	1.515	0.376
Cluster-12329.54345	hypothetical protein BRADI_2g44856v3	1.685	0.002	1.802	0.002	0.879	0.498	0.909	0.598
Cluster-12329.76277	hypothetical protein BRADI_2g52317v3	1.974	0.024	1.786	0.048	1.259	0.505	1.396	0.511

 doi:10.20944/preprints202501.1406.v1

Cluster-12329.49150	hypothetical protein BRADI_4g08097v3	0.647	0.004	0.601	0.004	0.672	0.065	0.588	0.018
Cluster-12329.70711	hypothetical protein C2845_PM01G12550	2.075	0.001	1.812	0.012	0.469	0.242	0.856	0.731
Cluster-12329.57642	hypothetical protein OsI_09291	1.758	0.002	1.378	0.029	1.135	0.353	1.321	0.074
Cluster-12329.47167	hypothetical protein OsI_16658	0.473	0.015	0.523	0.023	0.435	0.018	0.566	0.095
Cluster-12329.46264	NADH--cytochrome b5 reductase 1	0.772	0.006	0.752	0.006	0.663	0.026	0.561	0.008
Cluster-12329.40903	papain-like cysteine proteinase	0.083	0.014	0.106	0.003	0.336	0.068	0.308	0.060
Cluster-12329.42451	phospho-2-dehydro-3-deoxyheptonate aldolase 1, chloroplastic	0.390	0.025	0.466	0.007	0.808	0.402	0.745	0.300
Cluster-12329.45920	phospholipid-transporting ATPase 3 isoform X1	0.315	0.001	0.293	0.000	0.913	0.563	1.120	0.253
Cluster-12329.53668	plastid glutamine synthetase isoform GS2b	2.244	0.001	1.760	0.017	0.686	0.006	0.762	0.038
Cluster-12329.47790	polygalacturonase inhibitor	1.994	0.019	1.450	0.050	1.967	0.001	1.828	0.151
Cluster-12329.47853	polyol transporter 5-like	2.947	0.030	2.418	0.035	1.021	0.886	1.154	0.316
Cluster-12329.43728	predicted protein	1.400	0.019	1.475	0.035	0.821	0.253	0.750	0.107
Cluster-12329.45053	predicted protein	1.322	0.020	1.722	0.005	0.676	0.072	0.491	0.022
Cluster-12329.64971	predicted protein	0.353	0.007	0.584	0.022	0.464	0.091	0.577	0.287
Cluster-12329.45487	predicted protein	0.264	0.011	0.574	0.012	0.452	0.005	0.577	0.024
Cluster-12329.58094	predicted protein	0.390	0.049	0.528	0.046	0.668	0.175	0.886	0.763
Cluster-12329.50128	predicted protein	0.607	0.003	0.622	0.048	0.999	0.996	0.635	0.050
Cluster-12329.29002	predicted protein	2.032	0.018	1.662	0.048	1.854	0.017	1.761	0.033
Cluster-12329.19503	predicted protein, partial	1.585	0.007	1.277	0.020	0.899	0.739	0.601	0.215
Cluster-12329.50406	succinyl-CoA ligase subunit beta, mitochondrial	1.159	0.012	1.235	0.035	0.810	0.067	0.773	0.047

 doi:10.20944/preprints202501.1406.v1

Cluster-12329.44784	PREDICTED: sulfite oxidase	0.448	0.002	0.561	0.006	0.960	0.805	0.635	0.127
Cluster-12329.44784	PREDICTED: sulfite oxidase	0.754	0.037	0.698	0.026	0.909	0.066	0.803	0.038
Cluster-12329.27553	putativeUDP-rhamnose:rhamnosyltransferase 1	0.624	0.042	0.369	0.002	0.997	0.990	1.031	0.910
Cluster-12329.21291	pyridoxine/pyridoxamine 5-phosphate oxidase 1, chloroplastic	1.300	0.037	0.333	0.001	1.011	0.689	1.060	0.359
Cluster-12329.45221	S-adenosyl-L-homocysteine hydrolase	0.596	0.016	0.670	0.006	0.989	0.920	1.004	0.963
Cluster-12329.47122	subtilisin-like protease SBT1.7	0.447	0.006	0.679	0.023	0.620	0.176	0.394	0.083
Cluster-12329.33253	Threonine synthase 1, chloroplastic	1.474	0.001	1.264	0.031	1.787	0.000	1.557	0.099
Cluster-12329.58040	UDP-glycosyltransferase 72B1-like	0.335	0.014	0.471	0.007	0.279	0.002	0.200	0.015
Cluster-12329.39344	UGT80A24	2.163	0.001	1.986	0.001	0.790	0.058	0.980	0.909
Cluster-12329.23406	uncharacterized protein LOC100841867	0.320	0.042	0.398	0.026	0.339	0.255	1.033	0.957
Cluster-12329.37542	uncharacterized protein LOC109769744	1.988	0.004	1.349	0.033	1.295	0.207	2.294	0.077
Cluster-12329.45937	uncharacterized protein LOC109775963	1.316	0.003	1.287	0.005	1.049	0.399	1.168	0.015
Cluster-12329.46196	uncharacterized protein LOC541714 isoform X2	0.427	0.028	0.504	0.008	0.809	0.273	0.878	0.493
Cluster-12329.17719	universal stress protein PHOS32-like	0.529	0.005	0.543	0.010	0.543	0.007	0.411	0.003
Cluster-12329.41351	unnamed protein product	0.415	0.002	0.515	0.033	0.529	0.058	0.533	0.062
Cluster-12329.71832	unnamed protein product	3.554	0.001	4.595	0.003	2.040	0.172	3.491	0.001
Cluster-12329.46829	V-type proton ATPase catalytic subunit A	1.952	0.001	1.462	0.043	0.964	0.725	0.805	0.005

Table 6. JIA2 specifically expresses differential proteins under drought stres**.**

Protein	JIA2-2/2-1 FC	p-value	JIA2-2/2-1 FC	p-value	GO/KEGG Description
Cluster-12329.48386	0.41	0.0128	0.37	0.0071	xyloglucan galactosyltransferase MUR3
Cluster-12329.14848	0.45	0.0225	0.47	0.0253	xylan biosynthetic process
Cluster-12329.36881	2.12	0.0163	2.41	0.0127	vacuolar protein sorting-associated protein 54
Cluster-12329.43629	0.40	0.0257	0.44	0.0279	urease accessory protein
Cluster-12329.46978	2.87	0.0091	3.27	0.0029	tRNA guanosine-2′-O-methyltransferase
Cluster-12329.39756	0.48	0.0049	0.47	0.0289	transporter activity

 doi:10.20944/preprints202501.1406.v1

Cluster-12329.42106	0.44	0.0054	0.38	0.0017	transporter activity
Cluster-12329.45904	0.40	0.0262	0.33	0.0341	transporter activity
Cluster-12329.46297	0.40	0.0311	0.42	0.0077	transporter activity
Cluster-12329.46729	0.28	0.0025	0.24	0.0022	transporter activity
Cluster-12329.39937	0.44	0.0448	0.45	0.0448	transport
Cluster-12329.44647	0.36	0.0029	0.30	0.0007	transport
Cluster-12329.52083	0.50	0.0191	0.36	0.0094	transport
Cluster-12329.57154	2.49	0.0254	2.52	0.0062	transmembrane transport
Cluster-12329.39132	2.82	0.0022	2.76	0.0001	transketolase
Cluster-12329.33100	3.04	0.0000	2.49	0.0022	transaminase activity
Cluster-12329.36721	3.16	0.0489	4.92	0.0004	trafficking protein particle complex subunit 9
Cluster-12329.50073	2.32	0.0116	2.35	0.0058	threonine-type endopeptidase activity
Cluster-12329.56189	2.54	0.0360	2.83	0.0017	terpenoid biosynthetic process
Cluster-12329.59076	7.07	0.0000	11.86	0.0341	telomere maintenance
Cluster-12329.41271	0.32	0.0002	0.50	0.0021	sulfotransferase activity
Cluster-12329.38036	3.37	0.0376	3.03	0.0293	structural constituent of ribosome
Cluster-11888.0	2.32	0.0105	2.92	0.0013	structural constituent of ribosome
Cluster-12329.19614	2.05	0.0056	2.45	0.0030	structural constituent of ribosome
Cluster-12329.25578	2.51	0.0178	2.98	0.0225	structural constituent of ribosome
Cluster-12329.45480	2.97	0.0053	3.28	0.0298	structural constituent of ribosome
Cluster-12329.47059	2.18	0.0030	2.05	0.0220	structural constituent of ribosome
Cluster-12329.47776	2.20	0.0031	2.10	0.0135	structural constituent of ribosome
Cluster-12329.47836	2.64	0.0033	2.85	0.0408	structural constituent of ribosome
Cluster-12329.48202	3.17	0.0002	3.31	0.0082	structural constituent of ribosome
Cluster-12329.50106	3.38	0.0044	3.55	0.0090	structural constituent of ribosome
Cluster-12329.53055	2.33	0.0010	2.53	0.0029	structural constituent of ribosome
Cluster-12329.59685	4.38	0.0001	5.86	0.0005	structural constituent of ribosome
Cluster-12329.69623	5.79	0.0079	5.70	0.0031	structural constituent of ribosome
Cluster-16534.0	5.81	0.0001	7.93	0.0001	structural constituent of ribosome
Cluster-27122.0	2.08	0.0036	2.36	0.0131	structural constituent of ribosome
Cluster-12329.47699	0.34	0.0025	0.31	0.0025	structural constituent of cytoskeleton
Cluster-12329.60172	3.50	0.0099	3.37	0.0047	splicing factor, arginine/serine-rich 7
Cluster-12329.26481	2.28	0.0025	2.05	0.0057	spartin
Cluster-12329.35552	2.45	0.0146	2.30	0.0196	seryl-tRNA synthetase
Cluster-12329.35428	3.84	0.0005	6.42	0.0007	serine-type endopeptidase inhibitor activity
Cluster-12329.60990	3.15	0.0265	2.65	0.0318	serine-type endopeptidase inhibitor activity
Cluster-12329.48183	2.82	0.0136	2.95	0.0115	serine-type endopeptidase activity
Cluster-12329.49419	0.17	0.0002	0.29	0.0172	serine-type endopeptidase activity
Cluster-12329.38038	4.41	0.0236	4.96	0.0030	serine-type carboxypeptidase activity
Cluster-12329.53402	0.32	0.0205	0.27	0.0030	serine-type carboxypeptidase activity
Cluster-12329.43182	3.14	0.0463	3.70	0.0111	sequence-specific DNA binding
Cluster-12329.27710	2.56	0.0487	2.82	0.0174	SAP domain-containing ribonucleoprotein
Cluster-12329.52048	3.44	0.0002	3.86	0.0007	RNA processing
Cluster-12329.50126	4.30	0.0192	4.98	0.0090	RNA methylation
Cluster-12329.42822	2.09	0.0078	2.59	0.0029	RNA binding
Cluster-12329.21735	2.42	0.0011	2.64	0.0110	ribosome biogenesis protein BRX1
Cluster-12329.46311	3.19	0.0024	2.86	0.0054	ribosomal RNA-processing protein 12
Cluster-12329.51283	2.53	0.0011	2.67	0.0031	regulation of translation
Cluster-2168.0	0.21	0.0003	0.17	0.0021	pyroglutamyl-peptidase
Cluster-12329.62295	3.15	0.0046	3.02	0.0250	pseudouridine synthesis
Cluster-12329.58022	2.34	0.0055	2.98	0.0139	proton-transporting ATP synthase complex assembly
Cluster-12329.43644	0.28	0.0155	0.11	0.0010	proteolysis
Cluster-12329.35349	3.24	0.0096	3.24	0.0003	proteolysis
Cluster-12329.43809	0.44	0.0053	0.38	0.0119	proteolysis

 doi:10.20944/preprints202501.1406.v1

Cluster-12329.45109	0.34	0.0022	0.32	0.0026	proteolysis
Cluster-22035.1	0.34	0.0063	0.25	0.0182	proteolysis
Cluster-12329.31876	0.36	0.0093	0.47	0.0203	protein kinase activity
Cluster-12329.46753	0.45	0.0032	0.37	0.0049	protein kinase activity
Cluster-12329.50363	0.50	0.0006	0.48	0.0014	protein kinase activity
Cluster-12329.58642	0.18	0.0202	0.28	0.0347	protein kinase activity
Cluster-12329.45749	0.36	0.0000	0.39	0.0000	protein domain specific binding
Cluster-21280.0	4.95	0.0003	4.78	0.0000	protein dimerization activity
Cluster-12329.41964	0.42	0.0139	0.38	0.0064	protein binding
Cluster-12329.50319	0.38	0.0049	0.24	0.0020	protein binding
Cluster-12329.15022	3.21	0.0135	3.11	0.0323	protein binding
Cluster-12329.16346	2.42	0.0066	3.31	0.0017	protein binding
Cluster-12329.22341	3.19	0.0323	4.47	0.0000	protein binding
Cluster-12329.34668	3.41	0.0022	5.42	0.0006	protein binding
Cluster-12329.39776	3.32	0.0024	2.71	0.0066	protein binding
Cluster-12329.42509	0.37	0.0014	0.37	0.0404	protein binding
Cluster-12329.46138	0.42	0.0344	0.32	0.0298	protein binding
Cluster-12329.46986	4.39	0.0244	3.75	0.0472	protein binding
Cluster-12329.47845	0.29	0.0019	0.29	0.0046	protein binding
Cluster-12329.51162	2.29	0.0051	2.11	0.0135	protein binding
Cluster-12329.54023	2.00	0.0265	2.35	0.0458	protein binding
Cluster-12329.55764	3.46	0.0155	5.60	0.0231	protein binding
Cluster-12329.61573	0.19	0.0001	0.17	0.0001	protein binding
Cluster-12329.40181	0.29	0.0394	0.27	0.0377	prenylcysteine oxidase activity
Cluster-30010.0	4.93	0.0005	3.71	0.0145	phosphoglycerate mutase activity
Cluster-12329.33490	2.19	0.0038	2.63	0.0080	peroxin-5
Cluster-12329.14980	0.47	0.0025	0.30	0.0066	peroxidase activity
Cluster-12329.33750	0.49	0.0092	0.32	0.0065	peroxidase activity
Cluster-12329.36977	0.39	0.0007	0.30	0.0004	peroxidase activity
Cluster-12329.40101	0.12	0.0205	0.11	0.0032	peroxidase activity
Cluster-12329.42981	0.35	0.0040	0.28	0.0019	peroxidase activity
Cluster-12329.43312	0.40	0.0020	0.42	0.0111	peroxidase activity
Cluster-12329.43857	0.35	0.0195	0.30	0.0147	peroxidase activity
Cluster-12329.52051	0.28	0.0004	0.26	0.0004	peroxidase activity
Cluster-12329.52052	0.23	0.0064	0.23	0.0023	peroxidase activity
Cluster-12329.59924	0.44	0.0005	0.36	0.0026	peroxidase activity
Cluster-27561.0	0.34	0.0071	0.24	0.0039	peroxidase activity
Cluster-12329.73097	2.53	0.0027	2.16	0.0023	oxygen binding
Cluster-12329.45913	0.31	0.0057	0.26	0.0119	oxidoreductase activity
Cluster-12329.46857	0.49	0.0348	0.48	0.0075	oxidoreductase activity
Cluster-12329.49670	0.41	0.0042	0.36	0.0040	oxidoreductase activity
Cluster-12329.61877	0.48	0.0024	0.25	0.0003	oxidoreductase activity
Cluster-12329.60712	2.80	0.0073	2.50	0.0206	oxidation-reduction process
Cluster-12329.61816	0.36	0.0468	0.12	0.0183	omega-hydroxypalmitate O-feruloyl transferase
Cluster-12329.69497	6.09	0.0004	6.37	0.0302	nutrient reservoir activity
Cluster-12329.58725	0.44	0.0020	0.34	0.0091	nucleotide binding
Cluster-12329.45303	2.94	0.0025	2.37	0.0370	nucleosome
Cluster-22588.0	2.80	0.0306	3.57	0.0002	nucleosome
Cluster-12329.48442	2.19	0.0020	2.23	0.0063	nucleolar protein 56
Cluster-3608.0	9.51	0.0011	8.52	0.0244	nucleic acid binding
Cluster-12329.17354	2.50	0.0384	2.66	0.0020	nucleic acid binding
Cluster-12329.33078	2.48	0.0066	2.59	0.0049	nucleic acid binding
Cluster-12329.42921	2.03	0.0201	2.68	0.0052	nucleic acid binding
Cluster-12329.56144	2.22	0.0298	2.19	0.0301	nucleic acid binding
Cluster-12329.30577	2.29	0.0270	2.41	0.0255	nuclear pore complex protein Nup85
Cluster-12329.45111	2.90	0.0094	2.56	0.0402	nuclear GTP-binding protein
Cluster-12329.42303	0.27	0.0005	0.41	0.0415	nicotinate phosphoribosyltransferase
Cluster-12329.42372	0.18	0.0008	0.20	0.0007	negative regulation of translation

 doi:10.20944/preprints202501.1406.v1

Cluster-25204.0	2.13	0.0204	2.12	0.0172	NADH-ubiquinone oxidoreductase chain 6
Cluster-12329.47768	0.46	0.0241	0.32	0.0112	NADH dehydrogenase (ubiquinone) 1 beta subcomplex subunit 9
Cluster-12329.46665	0.30	0.0005	0.33	0.0052	NAD(P)H dehydrogenase (quinone)
Cluster-12329.46242	0.25	0.0114	0.29	0.0150	N-acetylneuraminate 9-O-acetyltransferase
Cluster-12329.51060	3.29	0.0006	2.19	0.0064	motor activity
Cluster-12329.23694	2.34	0.0108	2.86	0.0202	Molecular Function:protein binding
Cluster-12329.24463	0.43	0.0018	0.21	0.0001	Molecular Function:protein binding
Cluster-12329.41740	2.37	0.0148	2.66	0.0203	Molecular Function:catalytic activity
Cluster-12329.11672	2.09	0.0137	2.97	0.0005	mitochondrial phosphate transporter
Cluster-12329.17513	2.48	0.0084	2.45	0.0335	mitochondrial outer membrane translocase complex
Cluster-12329.45277	0.15	0.0007	0.21	0.0042	methyltransferase activity
Cluster-12329.45724	0.28	0.0205	0.37	0.0333	methionine adenosyltransferase activity
Cluster-12329.43185	0.47	0.0006	0.45	0.0066	metal ion transport
Cluster-12329.58884	2.12	0.0401	2.23	0.0164	metal ion binding
Cluster-12329.61926	0.49	0.0486	0.44	0.0408	metal ion binding
Cluster-12329.51889	2.66	0.0318	3.77	0.0013	metabolic process
Cluster-12329.57912	2.71	0.0028	3.09	0.0000	metabolic process
Cluster-12329.57969	0.35	0.0057	0.39	0.0087	metabolic process
Cluster-12329.63524	3.83	0.0002	3.66	0.0002	metabolic process
Cluster-12329.63525	5.34	0.0006	3.92	0.0001	metabolic process
Cluster-12329.63525	4.70	0.0004	4.28	0.0008	metabolic process
Cluster-30262.1	0.35	0.0006	0.26	0.0005	metabolic process
Cluster-12329.19357	5.21	0.0195	3.97	0.0005	membrane
Cluster-27225.0	3.33	0.0329	2.16	0.0201	membrane
Cluster-12329.40661	0.20	0.0335	0.32	0.0265	manganese ion binding
Cluster-12329.48850	0.40	0.0213	0.28	0.0068	malate metabolic process
Cluster-12329.55547	0.43	0.0035	0.25	0.0026	malate dehydrogenase
Cluster-12329.59603	7.03	0.0008	5.81	0.0023	malate dehydrogenase
Cluster-12329.23725	2.08	0.0393	3.50	0.0012	lipid transport
Cluster-12329.39105	0.35	0.0043	0.17	0.0023	lipid metabolic process
Cluster-12329.42824	0.30	0.0000	0.23	0.0001	lipid metabolic process
Cluster-12329.35244	4.75	0.0329	7.16	0.0043	large subunit ribosomal protein L7e
Cluster-12329.41754	2.18	0.0023	2.62	0.0002	large subunit ribosomal protein L7Ae
Cluster-12329.41497	2.51	0.0092	3.07	0.0034	large subunit ribosomal protein L27Ae
Cluster-12329.39606	6.27	0.0198	5.48	0.0012	large subunit ribosomal protein L24e
Cluster-12329.59427	3.41	0.0007	3.00	0.0174	lactoylglutathione lyase
Cluster-12329.48942	0.41	0.0094	0.24	0.0051	iron ion binding
Cluster-12329.48221	0.30	0.0334	0.29	0.0319	iron ion binding
Cluster-12329.51058	2.38	0.0021	2.20	0.0075	iron ion binding
Cluster-12329.17299	5.56	0.0011	4.36	0.0059	integral component of membrane
Cluster-12329.23588	3.13	0.0362	3.72	0.0099	integral component of membrane
Cluster-12329.26605	2.22	0.0038	3.14	0.0041	integral component of membrane
Cluster-12329.39422	0.32	0.0016	0.29	0.0013	integral component of membrane
Cluster-12329.44929	0.42	0.0010	0.28	0.0011	integral component of membrane
Cluster-12329.46026	2.32	0.0151	2.77	0.0063	inorganic diphosphatase activity
Cluster-12329.50264	0.40	0.0351	0.40	0.0409	hydroxymethylglutaryl-CoA synthase
Cluster-12329.53567	2.02	0.0092	2.34	0.0057	hydrolase activity
Cluster-12329.43240	7.43	0.0074	4.12	0.0137	heat shock 70kDa protein
Cluster-12329.29526	2.61	0.0012	3.69	0.0029	H/ACA ribonucleoprotein complex subunit 2
Cluster-12329.45696	0.25	0.0307	0.23	0.0144	GTPase activity
Cluster-12329.45717	0.43	0.0443	0.31	0.0270	GTPase activity
Cluster-20139.0	0.50	0.0036	0.39	0.0089	GTPase activity
Cluster-12329.45312	0.39	0.0052	0.38	0.0044	GTP binding
Cluster-12329.47784	2.76	0.0087	3.12	0.0005	GTP binding

 doi:10.20944/preprints202501.1406.v1

Cluster-12329.49630	0.41	0.0385	0.28	0.0173	GTP binding
Cluster-12329.15446	0.46	0.0411	0.18	0.0328	glutathione S-transferase
Cluster-12329.29554	0.46	0.0338	0.24	0.0198	FMN binding
Cluster-24056.0	0.24	0.0372	0.34	0.0136	FMN binding
Cluster-12329.36679	2.03	0.0084	2.13	0.0284	fatty acid metabolic process
Cluster-12329.68708	8.79	0.0003	6.95	0.0089	extracellular space
Cluster-12329.55067	0.12	0.0293	0.11	0.0281	exocyst
Cluster-12329.40027	4.64	0.0051	6.31	0.0056	essential nuclear protein 1
Cluster-12329.30167	0.40	0.0167	0.44	0.0110	endoplasmic reticulum
Cluster-12329.42162	0.47	0.0017	0.36	0.0100	endo-1,3(4)-beta-glucanase
Cluster-12329.32714	0.30	0.0068	0.11	0.0009	electron carrier activity
Cluster-12329.43095	0.37	0.0089	0.40	0.0095	electron carrier activity
Cluster-12329.45383	0.39	0.0020	0.22	0.0099	electron carrier activity
Cluster-12329.50014	0.34	0.0241	0.26	0.0176	electron carrier activity
Cluster-12329.51396	0.49	0.0416	0.33	0.0334	electron carrier activity
Cluster-12329.53251	0.40	0.0003	0.45	0.0005	electron carrier activity
Cluster-12329.63759	0.32	0.0305	0.18	0.0157	electron carrier activity
Cluster-12329.58928	2.58	0.0045	3.41	0.0285	DnaJ homolog subfamily C member 2
Cluster-12329.47118	2.34	0.0301	3.00	0.0497	DNA binding
Cluster-12329.50646	2.32	0.0000	2.08	0.0023	DNA binding
Cluster-12329.10108	6.05	0.0108	6.18	0.0076	defense response
Cluster-12329.32721	0.32	0.0024	0.14	0.0016	cytochrome-c oxidase activity
Cluster-12329.46264	0.44	0.0003	0.40	0.0014	cytochrome-b5 reductase
Cluster-12329.49622	0.46	0.0150	0.36	0.0035	cysteine synthase A
Cluster-12329.47550	2.02	0.0096	2.86	0.0032	cullin-associated NEDD8-dissociated protein
Cluster-12329.47555	7.02	0.0220	9.93	0.0054	chitinase activity
Cluster-12329.39096	2.81	0.0085	2.76	0.0042	chitinase
Cluster-12329.36403	0.42	0.0037	0.46	0.0425	cellular amino acid metabolic process
Cluster-12329.36404	0.27	0.0039	0.19	0.0046	cellular amino acid metabolic process
Cluster-12329.53200	0.32	0.0463	0.35	0.0467	catalytic activity
Cluster-12329.42675	0.50	0.0251	0.30	0.0185	catalytic activity
Cluster-12329.35194	0.16	0.0011	0.13	0.0014	catalytic activity
Cluster-12329.41051	0.39	0.0013	0.19	0.0001	catalytic activity
Cluster-12329.41231	0.47	0.0135	0.38	0.0334	catalytic activity
Cluster-12329.58241	2.97	0.0061	3.05	0.0088	catalytic activity
Cluster-12329.60324	12.28	0.0001	10.59	0.0001	catalytic activity
Cluster-12329.60324	6.31	0.0005	4.79	0.0030	catalytic activity
Cluster-12329.61956	0.25	0.0127	0.18	0.0403	catalytic activity
Cluster-12329.70108	8.16	0.0001	8.62	0.0000	catalytic activity
Cluster-12329.68563	0.29	0.0206	0.39	0.0266	carbohydrate metabolic process
Cluster-12329.29591	2.03	0.0030	4.49	0.0162	carbohydrate metabolic process
Cluster-12329.34933	2.81	0.0033	3.02	0.0219	carbohydrate metabolic process
Cluster-12329.43587	0.28	0.0001	0.23	0.0000	carbohydrate metabolic process
Cluster-12329.48578	0.44	0.0371	0.40	0.0496	carbohydrate metabolic process
Cluster-12329.51456	2.57	0.0170	2.88	0.0067	carbohydrate metabolic process
Cluster-12329.51985	0.36	0.0183	0.17	0.0317	carbohydrate metabolic process
Cluster-12329.53243	0.36	0.0060	0.28	0.0118	carbohydrate metabolic process
Cluster-12329.59871	0.19	0.0206	0.20	0.0212	carbohydrate metabolic process
Cluster-12329.61460	0.34	0.0023	0.23	0.0003	carbohydrate metabolic process
Cluster-12329.69576	0.38	0.0021	0.46	0.0048	carbohydrate metabolic process
Cluster-12329.48513	3.38	0.0004	2.95	0.0020	calcium ion binding
Cluster-12329.63459	2.17	0.0344	2.05	0.0229	calcium ion binding
Cluster-12329.36041	0.39	0.0035	0.43	0.0054	caffeoyl-CoA O-methyltransferase
Cluster-12329.21254	0.46	0.0232	0.26	0.0102	biosynthetic process
Cluster-12329.19475	2.32	0.0191	2.05	0.0111	Biological Process:cell redox homeostasis
Cluster-12329.49557	2.16	0.0114	2.39	0.0347	ATP-dependent RNA helicase DOB1
Cluster-12329.44150	2.20	0.0013	2.33	0.0100	ATP-dependent RNA helicase DBP3

 doi:10.20944/preprints202501.1406.v1

Cluster-12329.36548	0.34	0.0369	0.41	0.0383	ATP binding
Cluster-12329.39910	0.18	0.0089	0.13	0.0067	ATP binding
Cluster-12329.65472	0.47	0.0172	0.37	0.0052	ATP binding
Cluster-8220.0	0.34	0.0276	0.13	0.0291	aspartic-type endopeptidase activity
Cluster-12329.33762	0.22	0.0024	0.17	0.0022	aspartic-type endopeptidase activity
Cluster-12329.47560	2.51	0.0004	3.62	0.0473	aspartic-type endopeptidase activity
Cluster-12329.47580	0.49	0.0080	0.22	0.0013	aspartic-type endopeptidase activity
Cluster-12329.49924	0.31	0.0087	0.41	0.0116	aspartic-type endopeptidase activity
Cluster-12329.58062	0.43	0.0273	0.32	0.0446	aspartic-type endopeptidase activity
Cluster-12329.48665	2.31	0.0312	2.12	0.0102	asparagine synthase (glutamine-hydrolysing)
Cluster-12329.64984	0.40	0.0018	0.18	0.0002	amidase activity
Cluster-12329.47418	0.42	0.0004	0.41	0.0060	actin, other eukaryote
Cluster-12329.43923	0.45	0.0167	0.37	0.0141	actin binding
Cluster-12329.51553	0.37	0.0031	0.21	0.0003	actin beta/gamma 1
Cluster-12329.46649	0.37	0.0107	0.25	0.0048	acid phosphatase activity
Cluster-12329.54954	3.38	0.0006	2.63	0.0320	acid phosphatase activity
Cluster-12329.76839	0.35	0.0004	0.29	0.0012	acid phosphatase activity
Cluster-12329.26903	2.96	0.0006	2.77	0.0006	6-phosphofructokinase activity
Cluster-12329.48062	0.32	0.0051	0.27	0.0039	4-coumarate--CoA ligase
Cluster-12329.70084	2.63	0.0004	2.11	0.0187	4-alpha-glucanotransferase activity
Cluster-12329.52214	0.49	0.0342	0.25	0.0138	3-phosphoshikimate 1-carboxyvinyltransferase
Cluster-12329.33319	2.60	0.0164	2.92	0.0130	3-hydroxyisobutyryl-CoA hydrolase activity
Cluster-17679.0	2.02	0.0001	2.45	0.0000	1-pyrroline-5-carboxylate dehydrogenase
Cluster-10701.1	3.83	0.0172	5.11	0.0004	--
Cluster-12329.45692	0.45	0.0033	0.41	0.0028	--
Cluster-12329.12	0.43	0.0025	0.32	0.0086	--
Cluster-12329.15521	0.46	0.0293	0.38	0.0317	--
Cluster-12329.16465	2.81	0.0373	5.13	0.0242	--
Cluster-12329.19760	4.98	0.0022	6.54	0.0041	--
Cluster-12329.20993	3.82	0.0278	5.00	0.0146	--
Cluster-12329.21425	0.47	0.0023	0.26	0.0001	--
Cluster-12329.22132	2.83	0.0051	2.06	0.0416	--
Cluster-12329.24467	5.39	0.0001	6.15	0.0240	--
Cluster-12329.26112	2.72	0.0034	2.15	0.0499	--
Cluster-12329.30725	0.39	0.0245	0.16	0.0296	--
Cluster-12329.30855	0.33	0.0192	0.39	0.0190	--
Cluster-12329.31252	2.46	0.0419	15.22	0.0079	--
Cluster-12329.32559	2.00	0.0241	2.87	0.0202	--
Cluster-12329.33447	2.36	0.0060	2.27	0.0161	--
Cluster-12329.34089	2.03	0.0055	2.41	0.0016	--
Cluster-12329.34631	0.27	0.0001	0.18	0.0000	--
Cluster-12329.37085	0.37	0.0226	0.33	0.0384	--
Cluster-12329.37995	0.11	0.0119	0.24	0.0145	--
Cluster-12329.40468	0.46	0.0318	0.24	0.0156	--
Cluster-12329.40963	0.45	0.0022	0.21	0.0016	--
Cluster-12329.40989	2.99	0.0472	4.62	0.0085	--
Cluster-12329.41906	7.56	0.0001	6.54	0.0353	--
Cluster-12329.41956	6.01	0.0008	9.31	0.0266	--
Cluster-12329.42024	0.50	0.0204	0.42	0.0345	--
Cluster-12329.42053	0.34	0.0113	0.21	0.0041	--
Cluster-12329.42685	2.09	0.0018	2.25	0.0012	--
Cluster-12329.44022	2.01	0.0371	2.89	0.0033	--
Cluster-12329.44215	7.51	0.0198	5.86	0.0018	--
Cluster-12329.44647	0.41	0.0328	0.33	0.0242	--
Cluster-12329.44648	0.39	0.0017	0.24	0.0010	--

 doi:10.20944/preprints202501.1406.v1

Cluster-12329.44648	0.29	0.0018	0.32	0.0020	--
Cluster-12329.44802	0.41	0.0005	0.40	0.0044	--
Cluster-12329.44810	3.53	0.0073	3.62	0.0070	--
Cluster-12329.45397	2.46	0.0003	2.44	0.0000	--
Cluster-12329.45476	2.10	0.0290	3.18	0.0110	--
Cluster-12329.45721	2.84	0.0371	4.08	0.0124	--
Cluster-12329.45893	0.41	0.0104	0.32	0.0171	--
Cluster-12329.46781	0.42	0.0123	0.26	0.0052	--
Cluster-12329.48367	0.46	0.0180	0.45	0.0181	--
Cluster-12329.51534	0.30	0.0220	0.28	0.0188	--
Cluster-12329.51806	0.37	0.0030	0.16	0.0009	--
Cluster-12329.53646	0.25	0.0078	0.13	0.0200	--
Cluster-12329.53863	0.48	0.0359	0.36	0.0195	--
Cluster-12329.54583	3.24	0.0014	3.14	0.0027	--
Cluster-12329.54669	0.34	0.0011	0.39	0.0005	--
Cluster-12329.55286	0.19	0.0317	0.29	0.0432	--
Cluster-12329.55503	2.30	0.0049	2.24	0.0148	--
Cluster-12329.55504	4.14	0.0401	3.92	0.0005	--
Cluster-12329.55770	2.80	0.0096	3.73	0.0397	--
Cluster-12329.55856	2.20	0.0263	2.48	0.0195	--
Cluster-12329.56671	0.33	0.0117	0.36	0.0185	--
Cluster-12329.63149	0.19	0.0006	0.09	0.0001	--
Cluster-12329.63577	3.94	0.0436	3.01	0.0429	--
Cluster-12329.64664	2.64	0.0467	2.82	0.0048	--
Cluster-12329.65108	2.83	0.0018	3.37	0.0156	--
Cluster-12329.66452	3.06	0.0005	3.11	0.0014	--
Cluster-12329.68807	2.60	0.0273	2.80	0.0024	--
Cluster-12329.69143	4.48	0.0015	4.44	0.0120	--
Cluster-12329.75135	7.23	0.0051	6.71	0.0198	--
Cluster-2111.0	0.47	0.0487	0.26	0.0296	--

2.9. GO and KEGG Enrichment Analyses of DEPs

GO classification of DEPs indicated that under moderate stress, BA9 proteins were primarily enriched in the organic acid biosynthetic process, small molecule biosynthetic process, defense response, regulation of the cellular macromolecular biosynthetic process, and transferase activity involving acyl groups other than aminoacyl groups. Under severe stress, BA9 proteins were predominantly enriched in response to stimuli, response to stress, tetrapyrrole binding, enzyme inhibitor activity, and defense response. Under moderate stress, JIA2 DEPs were mainly enriched in the oxidation-reduction process, oxidoreductase activity, intracellular nonmembrane-bounded organelles, peptide metabolic processes, and response to stress. Under severe stress, JIA2 proteins were predominantly enriched in response to stimuli, intracellular nonmembrane-bounded organelles, structural molecular activity, structural constants of ribosomes, ribosomes, and peroxidase activity. These findings indicate that both oat cultivars experienced heightened biological, metabolic, and molecular functional responses under drought stress, with JIA2 undergoing more pronounced changes in cellular components compared to BA9.

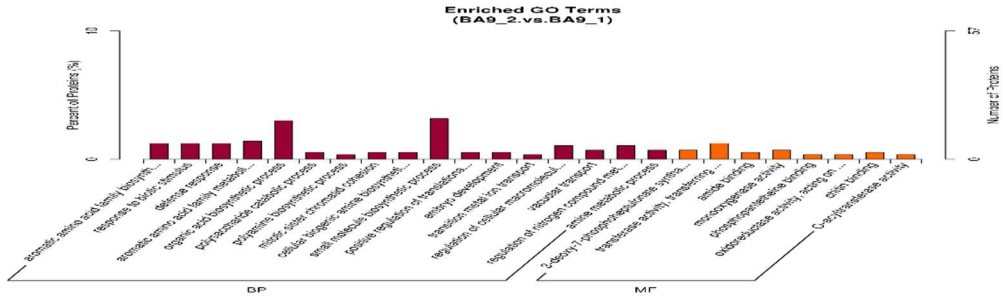

 doi:10.20944/preprints202501.1406.v1

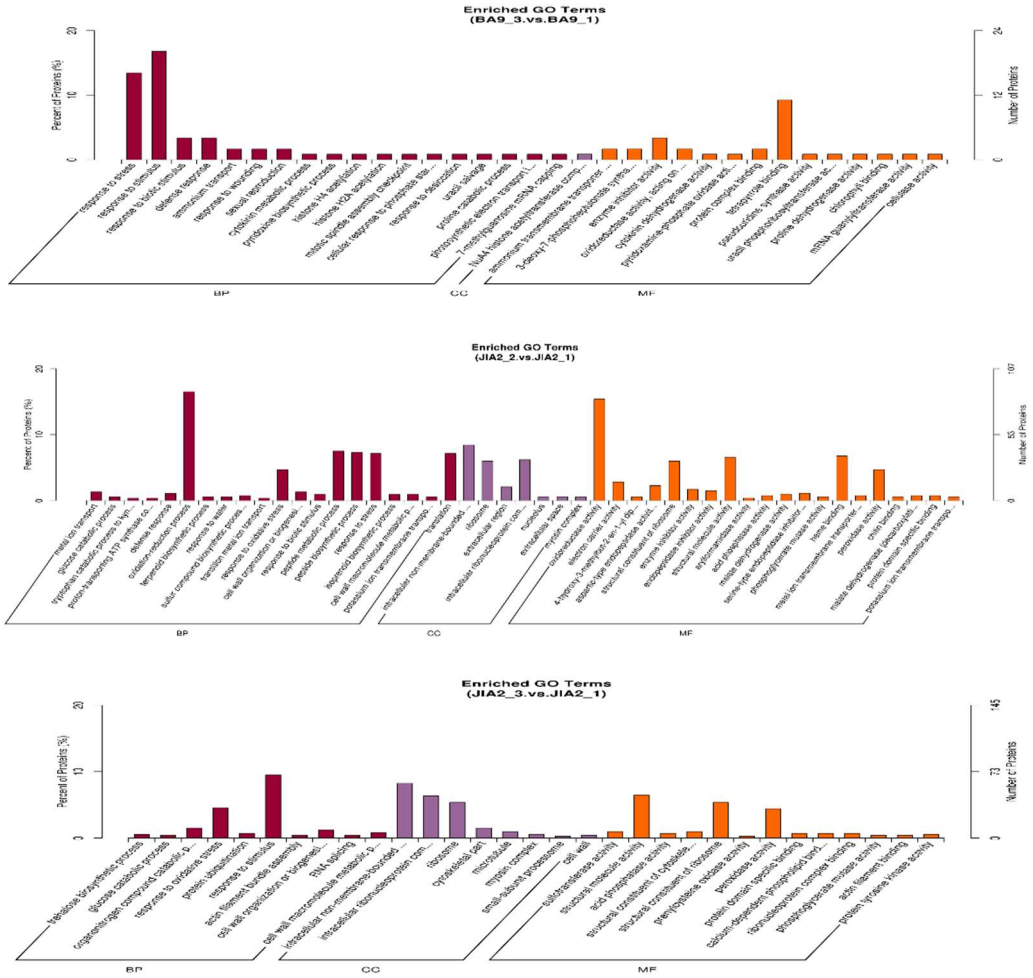

Figure 12. Analysis of GO Enrichment of Differentially Expressed proteins in Oats under Drought Stress.

We used the KEGG database to identify the main metabolic pathways associated with DEPs. Under moderate stress, the metabolic pathways associated with BA9 differential proteins mainly included the biosynthesis of secondary metabolites, amino acids, protein processing in the endoplasmic reticulum, and cysteine and methionine metabolism. Under severe stress, the metabolic pathways for BA9 differential proteins were primarily related to metabolic pathways, biosynthesis of secondary metabolites, phenylpropanoid biosynthesis, the MAPK signaling pathway in plants, and nitrogen metabolism. For JIA2 differential proteins, moderate stress primarily involved metabolic pathways: Biosynthesis of secondary metabolites, ribosomes, phenylpropanoid biosynthesis, and amino sugar and nucleotide sugar metabolism. Under severe stress, the metabolic pathways for JIA2 differential proteins were mainly associated with the biosynthesis of secondary metabolites, ribosomes, phenylpropanoid biosynthesis, starch and sucrose metabolism, amino sugar and nucleotide sugar metabolism, and alanine, aspartate, and glutamate metabolism.

 doi:10.20944/preprints202501.1406.v1

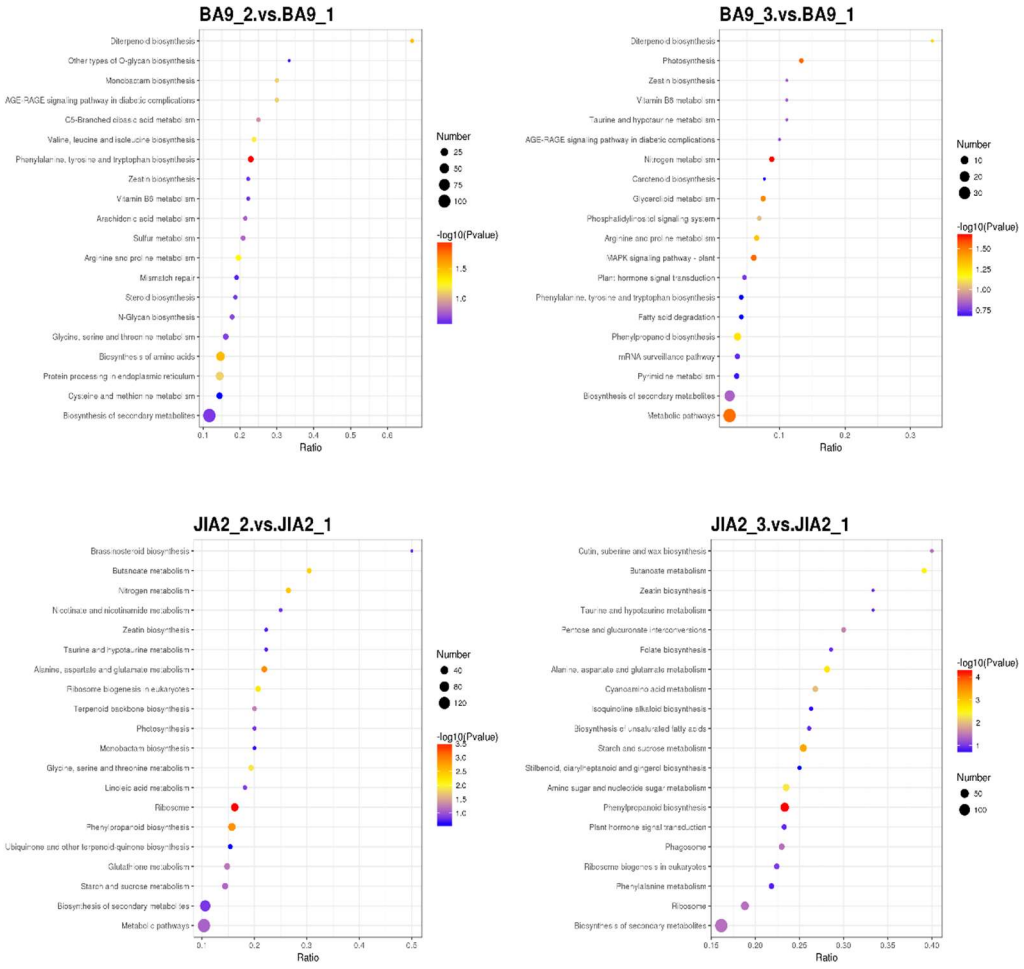

Figure 13. Analysis of KEGG enrichment of differentially expressed proteins in oats under drought stress**.**

2.10. Transcriptomic and Proteomic Correlation Analysis of Oat Response to Drought Stress

Figure 14 presents the correlation analysis between transcriptomics and proteomics. Compared with CK, BA9 under moderate stress exhibited 1,064 DEGs and 977 DEPs, with 48 matched cor DEGs-DEPs. Under severe stress, BA9 displayed 1,325 DEGs and 200 DEPs, with 19 matched cor DEGs-DEPs. For JIA2, under moderate stress, 4,005 DEGs and 858 DEPs were identified, among which 179 were matched with cor DEGs-DEPs. Under severe stress, JIA2 presented 6,521 DEGs and 1,160 DEPs, with 246 matched cor DEGs-DEPs.

The KEGG functional enrichment results of the association analysis between DEGs and DEPs indicated that, compared with CK, most DEGs and DEPs in BA9 were upregulated under moderate stress. Some DEGs and DEPs were downregulated, while a few exhibited opposing expression trends. The main pathways involved included metabolic (Cluster-12329.10917: V-type proton ATPase subunit; Cluster-12329.54954: assuming protein BRADI_1g03920v3), biosynthesis of secondary metabolites (Cluster-12329.64079: 6-phosphofructokinase 2; Cluster-12329.46310: Cytochrome P450 84A1; Cluster-12329.54450: peroxidase), and arginine and proline metabolism (Cluster-12329.60427: assuming protein BRADI_2g54920v3). Under severe stress, the number of DEGs and DEPs associated with the upregulation and downregulation of BA9 was roughly equal, with a relatively smaller total number. These primarily involved metabolic pathways (Cluster-12329.46928: β-glucosidase 4; Cluster-12329.60427: assuming protein BRADI_2g54920v3) and plant signal transduction pathways (Cluster-12329.35737: Abscisic acid receptor PYL2), as depicted in Figure 15.

 doi:10.20944/preprints202501.1406.v1

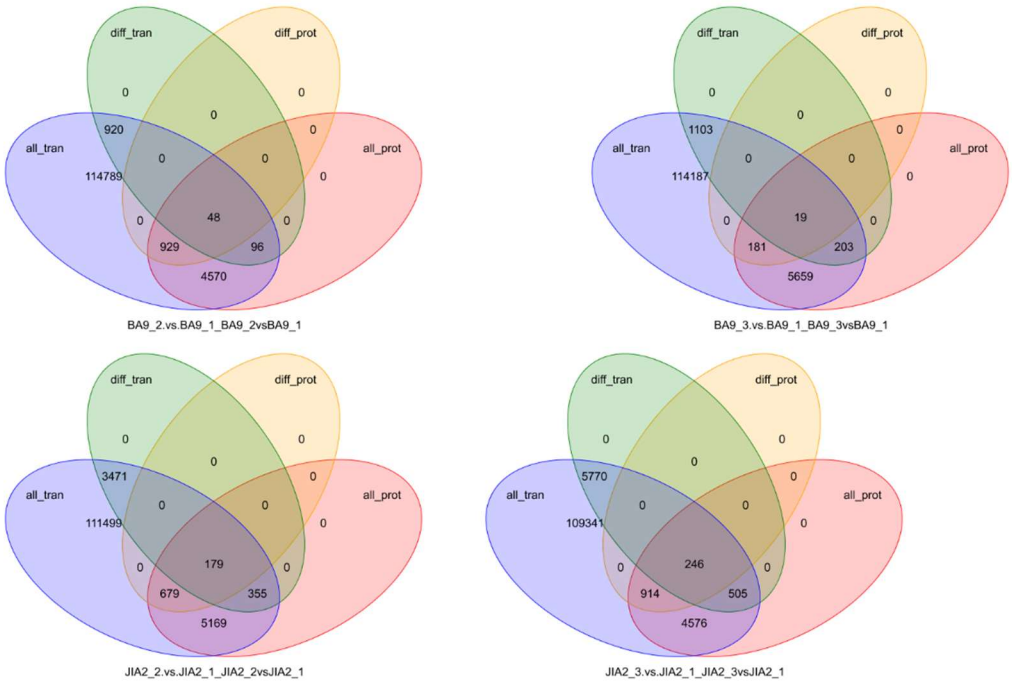

Figure 14. Differentially expressed genes and protein association analysis of two oats under drought stress.

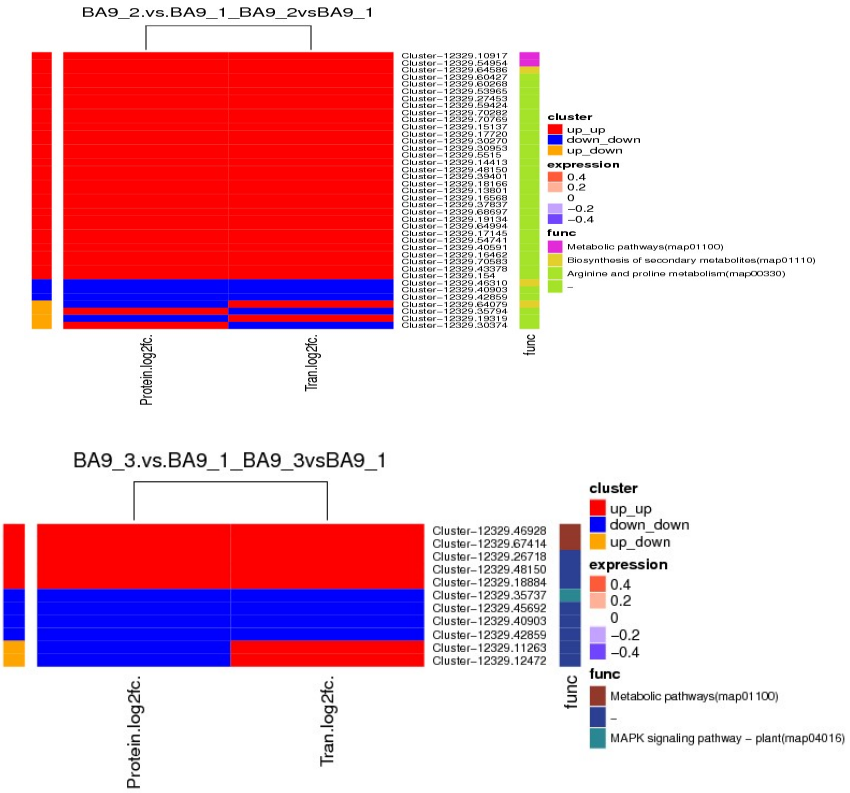

Figure 15. BA9 differentially expressed genes and protein association analysis under drought stress KEGG annotation.

Compared with CK, JIA2 under moderate stress exhibited 80 matched upregulated DEGs and DEPs, primarily associated with metabolic pathways, including Cluster-12329.52078 (peroxidase 7), Cluster-12329.10917 (V-type proton ATPase subunit), Cluster-12329.27420 (peroxidase P7), Cluster-12329.59603 (NADP-dependent malate enzyme), Cluster-12329.41740 (1,4-alpha-glucan branching enzyme 2), Cluster-12329.45206 (potential alpha trehalose phosphate synthase), Cluster-12329.36823

 doi:10.20944/preprints202501.1406.v1

(blunt leaf alcohol 14-α-demethylase), Cluster-12329.35358 (3-phosphoglycerol 2-O-acyltransferase 6), and Cluster-12329.43587 (fructan exonuclease). Additional pathways included biosynthesis of secondary metabolites (Cluster-12329.16474: NAD(P)H dehydrogenase FQR1) and ribosome biogenesis in eukaryotes (Cluster-12329.48442). Furthermore, 59 matched DEGs and DEPs were downregulated, mainly involving metabolic pathways such as glutathione metabolism (Cluster-12329.49095: protein IN2-1), plant-pathogen interactions (Cluster-12329.47252: calcium-dependent protein kinase 13; Cluster-12329.42554: Predictive protein), linoleic acid metabolism (Cluster-12329.44747: lipoxygenase), nitrogen metabolism (Cluster-12329.48919), and phagosome (Cluster-12329.51553). Additionally, a few matched DEGs displayed protein expression trends in the opposite direction.

Under severe stress, JIA2 exhibited 98 matched upregulated DEGs and DEPs, mainly associated with metabolic pathways, including Cluster-12329.59605 (NADP-dependent malate enzyme), Cluster-12329.58994 (hypothesized aldehyde dehydrogenase BIS1), Cluster-12329.63525 (mitochondrial succinate semialdehyde dehydrogenase), and Cluster-12329.59603 (NAD-dependent malate enzyme). Key pathways included starch and sucrose metabolism (Cluster-12329.47216: alpha glucan phosphorylase, H isoenzymes; Cluster-12329.35240: β-glucosidase 30; Cluster-12329.35438: hexokinase-7; Cluster-12329.68807: starch synthase 1; Cluster-12329.41740: 1,4-alpha glucan branching enzyme 2; Cluster-12329.99020: sucrose synthase 4), biosynthesis of secondary metabolites (Cluster-12329.36823: blunt leaf alcohol 14-α-demethylase; Cluster-12329.35914: short-chain dehydrogenase/reductase 2b; Cluster-12329.82252: 3-phosphoglyceraldehyde dehydrogenase), linoleic acid metabolism (Cluster-12329.99020: sucrose synthase 4), pyruvate metabolism (Cluster-12329.9902), lactase glutathione lyase (Cluster-12329.59424), and amino and nucleotide sugar metabolism (Cluster-12329.38074: hexamine-A; Cluster-12329.40415: 26 kDa endonuclease 1). Additionally, 80 matched DEGs and DEPs were downregulated, primarily linked to metabolic pathways such as Cluster-12329.40301 (sorbitol dehydrogenase isoform X1), starch and sucrose metabolism (Cluster-12329.45206: potential α-trehalose phosphate synthase; Cluster-12329.43587: fructan exonuclease), biosynthesis of secondary metabolites (Cluster-12329.48221: cytochrome P450; Cluster-12329.40101: cationic peroxidase SPC4; Cluster-12329.58512: ortho aminobenzoate synthase α2 subunit; Cluster-12329.42981: peroxidase 50; Cluster-12329.44161: DSL esterase/lipase At5g45910), phagosomes (Cluster-12329.51553), plant hormone signal transduction (Cluster-12329.57977: potential serine/threonine protein kinase At4g35230; Cluster-12329.50363: predicted protein), amino sugar and nucleotide sugar metabolism (Cluster-12329.33912: α-L-arabinofuranosidase 1; Cluster-12329.59871: hypothesized protein BRADI_2g55620v3), and nitrogen metabolism (Cluster-12329.45198: Nitrate transporter protein). A small number of matched DEGs also exhibited opposite protein expression trends.

Based on the correlation between DEGs and DEPs, four types of interacting DEPs were identified in the gene-protein interaction network analysis of the drought-resistant cultivar JIA2 under severe stress compared with CK. These proteins are mainly involved in plant hormone signal transduction, biosynthesis of secondary metabolites, carbohydrate metabolism, and metabolic pathways. Specific examples include the following:

(1) Cluster-12329.57977; Orf1 (serine/threonine protein kinase): associated with Cluster-12329.44642; Orf2, Cluster-12329.42764; Orf1, Cluster-12329.42435; Orf1, and Cluster-12329.31723. These proteins are involved in functions such as protein kinase activity. Cluster-12329.43859; Orf1 (histidine kinase): linked to Cluster-12329.46160; Orf1, Cluster-12329.49659; Orf1, Cluster-12329.46332; Orf1, Cluster-12329.46969; Orf2, Cluster-12329.35694; Orf2, Cluster-12329.47729; Orf2, Cluster-12329.48352; Orf1, and Cluster-12329.55239. These proteins are primarily involved in functions such as protein kinase, catalytic activity, glutamine synthetase, oxidoreductase activity, ATP binding, DNA binding, transcription, and thioredoxin.

(2) Cluster-12329.60427; Orf1 (glutamate 5-kinase) plays a key role and is associated with Cluster-12329.46488; Orf1 (hexokinase-2), Cluster-12329.52423; Orf1, Cluster-12329.55547; Orf2 (NADP-dependent malate enzyme), and Cluster-12329.47983; 51 proteins, including Orf1 (aspartate

 doi:10.20944/preprints202501.1406.v1

and glutamate aminotransferase), Cluster-12329.35444, and Cluster-12329.63308. These proteins are involved in functions including transmembrane transport, redox processes, amino acid transport and metabolism, and copper and metal ion binding. Cluster-12329.70108 (pyruvate decarboxylase) is associated with Cluster-12329.39132; Orf1 (ketotransferase), Cluster-12329.48465; Orf1 (aspartate aminotransferase), Cluster-12329.47267; Orf1 (pyruvate decarboxylase), Cluster-12329.55539; Orf1 (soluble acid converting enzyme), and Cluster-12329.99591; 20 proteins, including Orf2 (fructosyltransferase). These are primarily involved in carbohydrate transport and metabolism, amino acid transport and metabolism, energy production and conversion, and sugarcane candy glycosyltransferase. Cluster-12329.82252; Orf1 (phosphoglyceraldehyde dehydrogenase) was associated with Cluster-12329.43257; Orf1 (eukaryotic translation initiation factor).

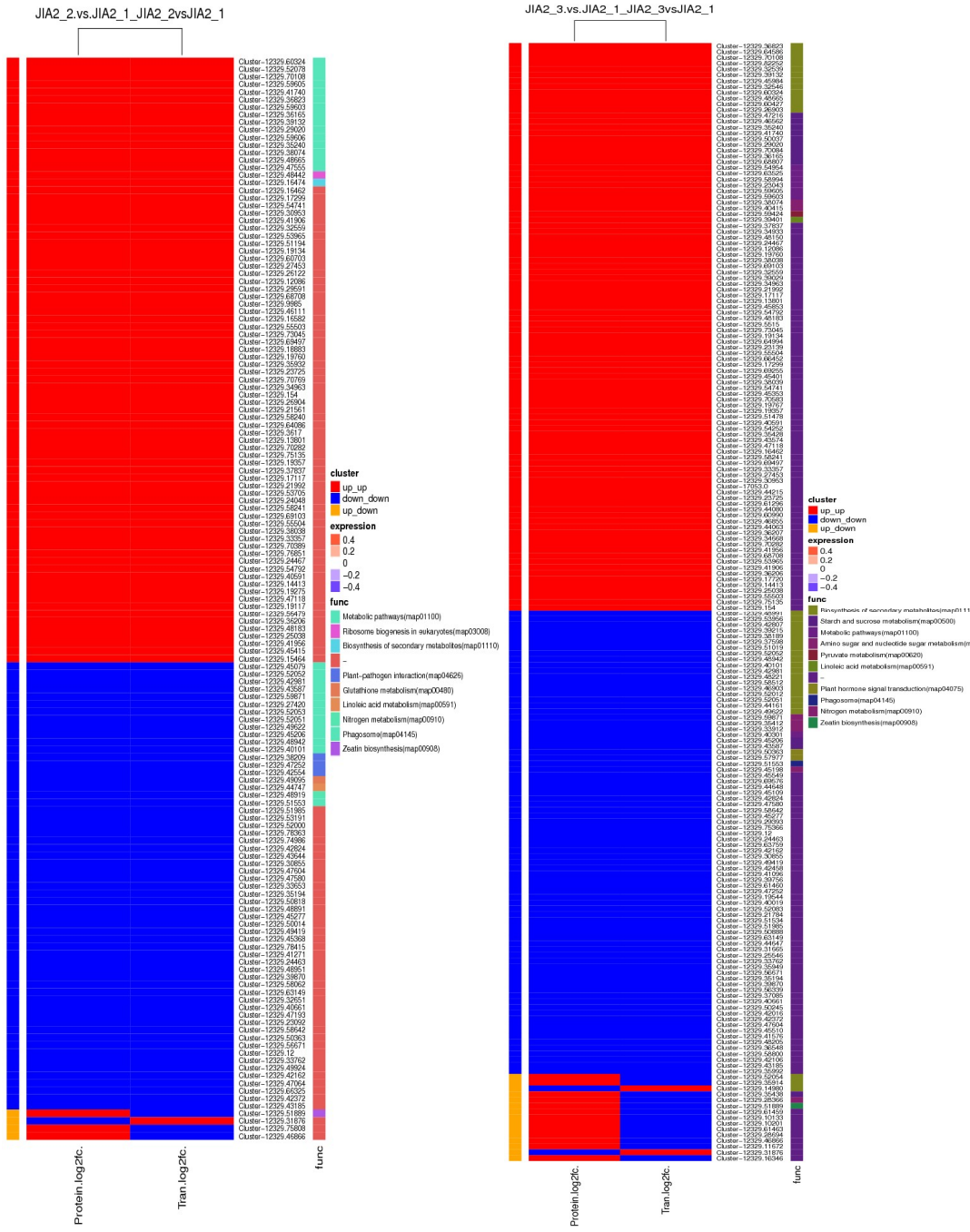

Figure 16. JIA2 differentially expressed genes and protein association analysis under drought stress KEGG annotation.

 doi:10.20944/preprints202501.1406.v1

(3) Cluster-12329.29020; Orf1 (sucrose synthase 4) plays a key role and is associated with Cluster-12329.42345; Orf1 (serine/threonine protein kinase SAPK8 isoform X1), Cluster-12329.46332; Orf1 (serine/threonine protein kinase STY13), Cluster-12329.45053; Orf1 (UDP pyrophosphate synthase), Cluster-12329.68807; Orf1 (starch synthase 1), and Cluster-12329.32559; Orf1 (α-glucosidase), among 39 proteins. These are primarily associated with protein kinase activity, carbohydrate transport and metabolism, and starch and sucrose metabolism. Cluster-12329.35240; Orf1 (β-glucosidase) is associated with Cluster-12329.43809; Orf2 (aminopeptidase M1-B), Cluster-12329.43240, Cluster-12329.32231; Orf1 (aldose 1-isomerase), Cluster-12329.68563; Orf1, Cluster-12329.36207; Orf1 (anthocyanin 3-O-glucosyltransferase), Cluster-12329.32253; Orf1 (Xet2 protein), among 16 proteins. These are mainly involved in protein hydrolysis, heat shock proteins, glycolysis, carbohydrate transport and metabolism, flavonoid glycosyltransferases, and xylose glycosyltransferases. Cluster-12329.36165; Orf1 (1-phosphate glucosyltransferase) is associated with Cluster-12329.25280; Orf1, Cluster-12329.48578; Orf2 (glycerol kinase), Cluster-12329.43732; Orf1 (6-phosphogluconate lactonase), Cluster-12329.41051; Orf1 (cinnamoyl CoA reductase), Cluster-12329.47992; Orf1 (trehalose-6-phosphate synthase 6), among 16 proteins. The functions are primarily associated with oxidoreductase activity, energy production and conversion, carbohydrate metabolism, catalytic activity, and trehalose biosynthesis process.

(4) Cluster-12329.62359; Orf1 (DNA primer subunit) was associated with Cluster-12329.23043; Orf1, Cluster-12329.46189; Orf1 and Cluster-12329.47118 (DNA Topoisomerase II), forming three proteins primarily involved in purine metabolism, chromosome separation ATPase, replication, recombination, and repair. Cluster-12329.59605; Orf1 (NADP-dependent malate enzyme) was associated with Cluster-12329.51283; Orf1, Cluster-12329.61956; Orf1, Cluster-12329.45169; Orf2 (protein RCF3 containing RNA binding KH domain), Cluster-12329.44534; Orf2 and 17 other proteins. These proteins are mainly associated with signal transduction mechanisms, energy production and conversion, nucleic acid binding, and redox processes. Cluster-12329.54954; Orf1 and Cluster-12329.54954; Orf2 are associated with Cluster-12329.20993; Orf1 (phosphoglycolic acid phosphatase 2) and Cluster-12329.42172; Orf1, primarily involving nucleotide transport and metabolism.

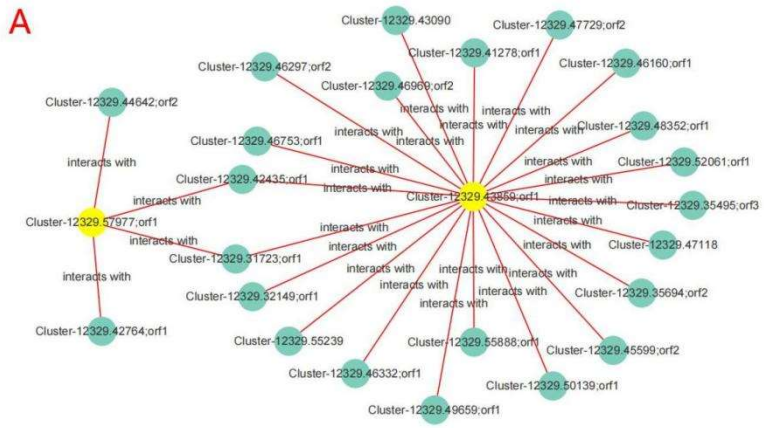

 doi:10.20944/preprints202501.1406.v1

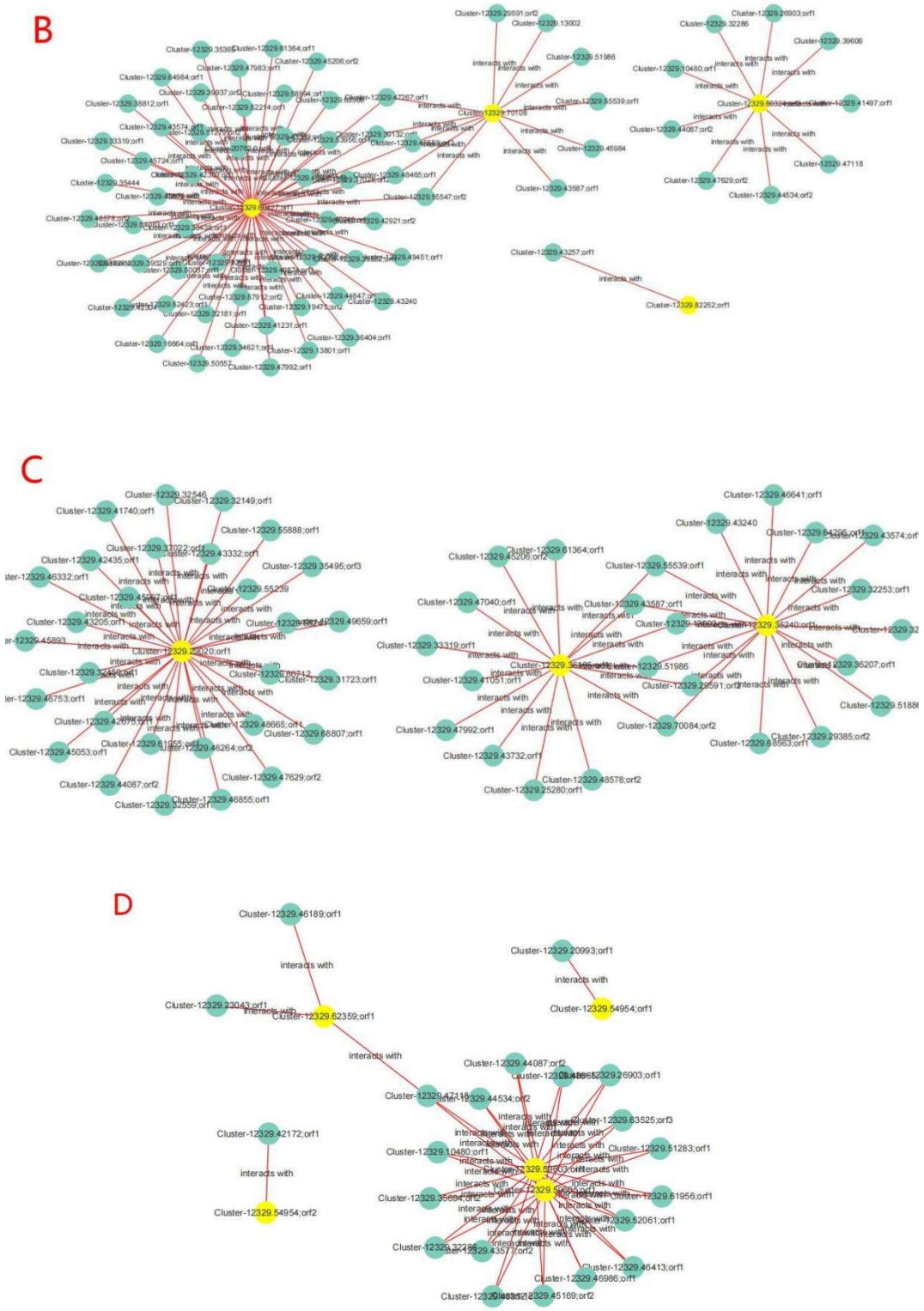

Figure 17. Mapping of key cor-DEGs-DEPs genes and protein networks.

Note: A, B, C, and D respectively represent cor-DEGs-DEPs, which belong to plant hormone signal transduction, secondary metabolite biosynthesis, carbohydrate metabolism process and metabolic pathway function.

 doi:10.20944/preprints202501.1406.v1

2.11. Validation of Key cor-DEGs-DEPs via qRT-PCR

To analyze the expression patterns of related genes, 13 key cor DEGs-DEPs from four key pathways in drought-resistant cultivar JIA2 were selected for qRT-PCR analysis. Two genes involved in plant hormone signaling transduction were downregulated. Two genes related to the biosynthesis of secondary metabolites and three genes associated with carbohydrate metabolism processes were upregulated. Additionally, four genes related to metabolic pathways were upregulated. The expression trends of these genes aligned with those of their corresponding proteins.

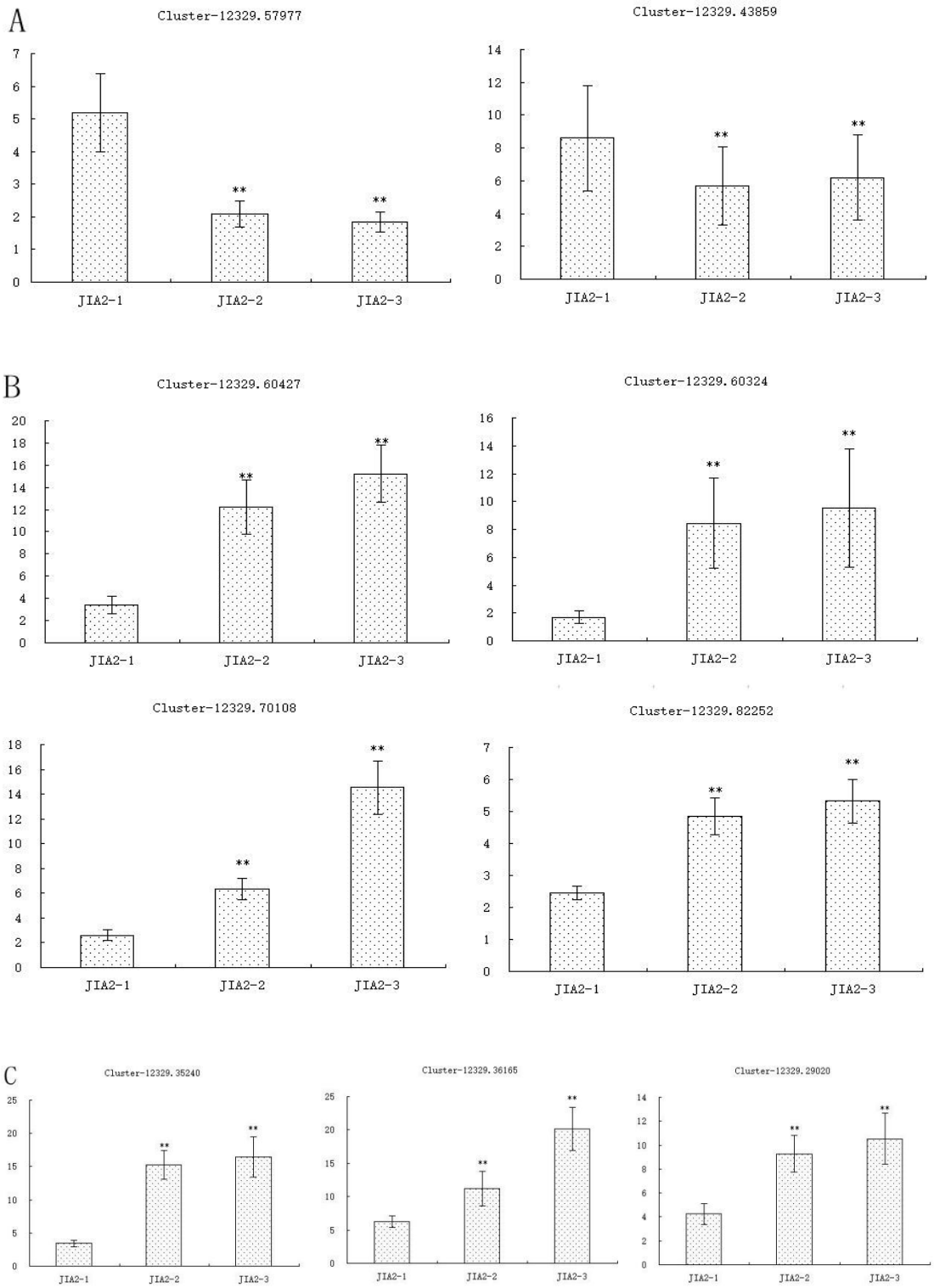

 doi:10.20944/preprints202501.1406.v1

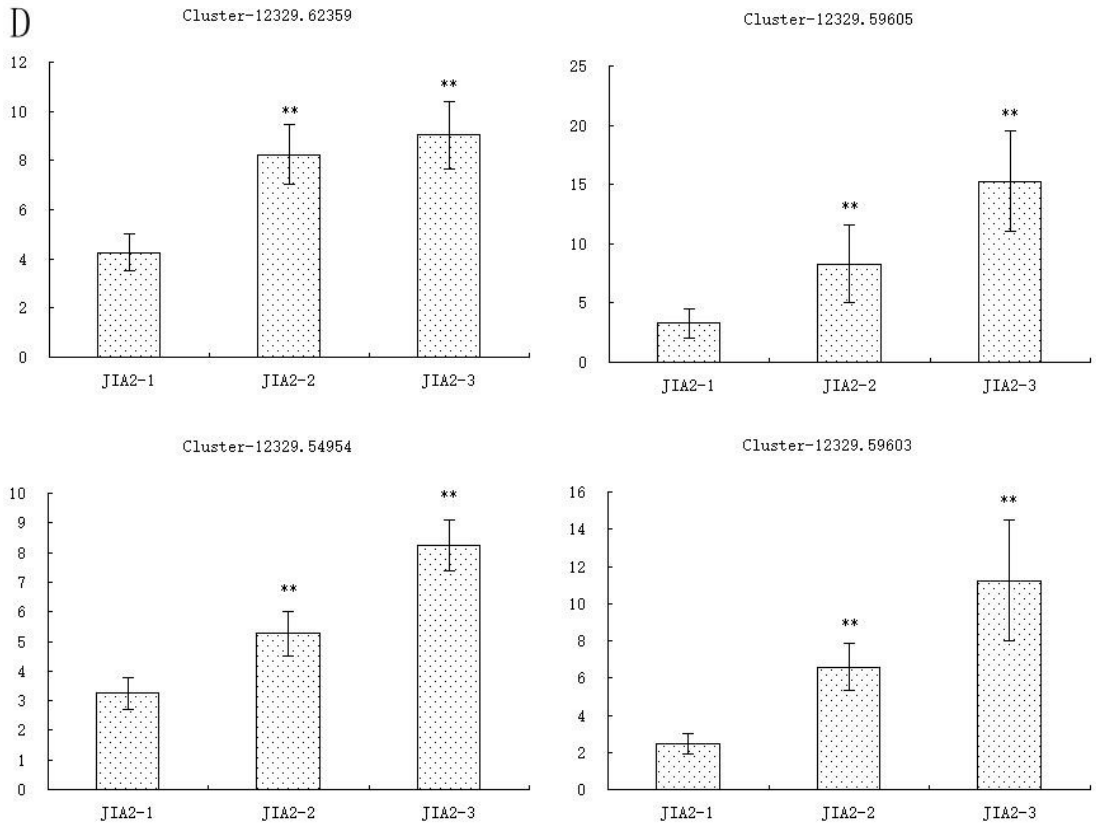

Figure 18. QRT-PCR expression of 13 target genes**.** Note: A, B, C, and D respectively represent cor-DEGs-DEPs, which belong to plant hormone signal transduction, secondary metabolite biosynthesis, carbohydrate metabolism process and metabolic pathway function.

Table 7. Primers used in real-time quantitative reverse transcription PCR (qRT-PCR) experiment**.**

Gene	Sequence (5′ to 3′)	Length(bp)
Cluster-12329.57977	F: CTCCTCACGCTTCATGGGTT R: TACGAGGTTGGGAGCCTTCT	280
Cluster-12329.43859	F:CGCCGACGAGATCTTCCAAA R:AGAATTGGAGGCAGTCCCAC	269
Cluster-12329.60427	F:AGGGGAGGTGACGAAGAGG R:CTCCTCGACGCCTGCAAC	170
Cluster-12329.60324	F:TCCTGAAGCAGAAGCAGAGC R:GATCTCTCCAGCAGTCCGTC	104
Cluster-12329.70108	F:GAGGGGAAGTGGAGGGAAGA R:CCCCCAAAACAGAAATGGCG	170
Cluster-12329.82252	F:CGCAGCTGAGTACAGATCGA R:GGCTTTGATTTGGTTCCCCG	255
Cluster-12329.35240	F:AGCTCACACAGGTTGTAGGC R:CCACCGCCGATTGGAATAGA	158
Cluster-12329.36165	F:TGAAGGAACAGAGCTGGCAG R:GGATGACACGGTGGAGGATC	216
Cluster-12329.29020	F:AGGTTTCCTCTGTTCTGGCT R:GGCTCTCGTACTGTCCAACA	263
Cluster-12329.62359	F:GCTCTCGACGCCCAATGTAT R:GCAGTACGCACAGTCGATCT	251
Cluster-12329.59605	F:AGATCCTCACGCTGCACTTC R:ACCAGAACAGGCTGAGCATC	227

 doi:10.20944/preprints202501.1406.v1

Cluster-12329.54954	F:TCACCCCGCTTCATTCTTCT R:AGCCTTGCACGGTACCATAG	257
Cluster-12329.59603	F:GTGGAAGGTCGTGAAGCTGA R:CCTCCACCACTTCACTCACC	116
actin	F: CCAATCGTGAGAAGATGACCC R: CACCATCACCAGAATCCAACA	135

3. Discussion

3.1. Correlation Analysis Revealed Key Metabolic Pathways of Oats in Response to Drought Stress

Proteomics is widely utilized to comprehensively examine protein changes under stress, uncover their mechanisms of action, and identify potential biomarkers. However, the number of related studies remains limited[21], potentially due to higher sensitivity of RNA-seq detection being more sensitive than protein detection or due to factors such as post-transcriptional and post-translational modifications or protein-regulated degradation[22]. To further investigate the regulatory mechanisms of the two oat cultivars under drought stress, this study interpreted the effects of drought stress through an in-depth combined analysis of transcriptome and proteome under drought stress conditions. This approach offers the advantage of establishing robust connections between datasets by comparing and reusing the same samples across multiple omics and biological replicates. The findings indicate that drought stress significantly alters the metabolic pathways in oat roots, including the biosynthesis of secondary metabolites, plant hormone signal transduction, and carbohydrate metabolism processes. Correlation analysis of transcriptomics and proteomics revealed significant molecular-level changes in the drought-resistant cultivar JIA2 and the sensitive cultivar BA9, aligning with previous findings on their growth responses under drought stress.

3.2. Carbohydrate Metabolism

Carbohydrate metabolism encompasses numerous biochemical processes essential for the synthesis, decomposition, and interconversion of carbohydrates in organisms, significantly influencing plant growth and stress responses[23]. The DEGs and DEPs identified in this study are involved in various carbohydrate metabolism, with the highest number associated with “starch and sucrose metabolism.” The carbon assimilation process primarily facilitates the synthesis of osmoregulatory substances, while starch degradation into glucose contributes to osmoregulation, enabling plants to resist or adapt to drought stress[24]. In the drought-resistant cultivar JIA2, the expression levels of soluble sugar metabolism-related genes exhibited significant changes, with upregulation and downregulation suggesting that drought stress promotes starch degradation and soluble sugar accumulation, redirects carbon flow within cells, and supplies energy for drought-resistant and adaptation. Results from association analysis and protein-gene network mapping further highlighted the critical roles of proteins such as Cluster-12329.29020; Orf1 (sucrose synthase 4), Cluster-12329.68807; Orf1 (starch synthase 1), Cluster-12329.32559; Orf1 (α-glucosidase) and Cluster-12329.36165; Orf1 (1-phosphate glucosyltransferase) in oat adaptation to drought stress. Similar findings were reported in studies examining the expression changes of key enzyme genes involved in insoluble and soluble sugar metabolism in tea plants under drought stress[24].

3.3. Amino Acid Metabolism and Secondary Metabolism

Studies have identified that DEGs in Populus euphratica under drought stress are associated with amino acid metabolism and transport, with plasma membrane transporters facilitating amino acid transport[24]. In this experiment, correlation analysis indicated that the biosynthesis of metabolites, amino sugar, and nucleotide sugar metabolism pathways were significantly enriched only in the drought-resistant cultivar JIA2. This indicates that these metabolic pathways play an important role in the drought resistance of JIA2. Furthermore, most of the DEGs and DEPs involved

 doi:10.20944/preprints202501.1406.v1

in glutamate and aspartate metabolism in JIA2, such as Cluster-12329.60427 (glutamate 5-kinase) and Cluster-12329.47983 (aspartate and glutamate aminotransferase), exhibited both upregulation and downregulation under drought stress. These findings suggest that glutamate and aspartate metabolism may be key regulatory pathways in oat response to drought stress.

Drought stress exerts a significant impact on the synthesis of secondary metabolites. DEGs associated with the metabolic pathways of various secondary metabolites, particularly key regulatory genes in the biosynthesis pathways of flavonoids and phenylpropanoids, were identified in the transcriptome of tea plants under drought stress[25]. The findings of this experiment align with previous studies. In oat roots, drought stress significantly affects the phenylpropanoid biosynthesis pathway, with most genes, including 4-coumaric acid CoA ligase, 3-hydroxyisobutyrylCoA hydrolase, caffeoyl CoA O-methyltransferase, peroxidase family proteins, and cationic peroxidase, exhibiting significantly higher downregulation than upregulation expression. Under drought stress, plants adapt metabolically through complex recombination across multiple metabolic pathways. Cytoplasmic enzyme activity related to defense and secondary metabolism in the root system undergoes significant changes under abiotic stress[26,27]. This experiment identified several proteins, including chitinase, 3-hydroxyisobutyryl-CoA hydrolase, 1-pyrroline-5-carboxylic acid dehydrogenase, 4-coumaric acid CoA ligase, keto transferase, and sulfotransferase, as significantly differentially expressed only in the drought-resistant cultivar JIA2. These stress-induced proteins play important roles in secondary metabolism and key stress adaptation mechanisms, enhancing the drought resistance of oat.

3.4. Plant Hormone Signaling and Transcription Factors

Plant hormones are closely linked to various abiotic stresses and play an important role in rehydration after drought stress[12,28]. Drought stress induced the expression of most genes involved in ABA biosynthesis in the root system of the tested oats, including sucrose non-fermenting 1-related kinase, abscisic acid receptor, serine/threonine kinase SAPK1 protein, and abscisic acid receptor. Additionally, protein phosphatase 2C protein exhibited both upregulation and downregulation, while ABA-responsive element binding factors were downregulated. These findings indicate that ABA is likely a key regulatory factor in oat response to drought stress[7,29]. Furthermore, the abscisic acid receptor PYL2 was specifically expressed in the sensitive cultivar BA9, whereas BR signaling kinase was significantly differentially expressed only in the drought-resistant cultivar JIA2.

AP2/ERF, MYB, NAC, bHLH, and WRKY transcription factors in the TF family play important roles in regulating abiotic stress tolerance in Arabidopsis and rice. This study observed no DEGs in BA9 under drought stress when compared with the Arabidopsis transcription factor database. Under moderate stress, JIA2 exhibited 3 upregulated and 9 downregulated DEGs in comparison to the database. These transcription factors were divided into 10 categories, mainly distributed as follows: MYB (2), WRKY (2), AP2 (1), GATA (1), and HSF (1). Under severe stress, JIA2 identified 5 upregulated and 12 downregulated DEGs, grouped into 12 categories, predominantly WRKY (3), MYB (2), HSF (2), bHLH (2), and GATA (1)[23]. In Populus euphratica, 19 TF families were identified, predominantly AP2/ERF and WRKY, followed by bZIP, NAC, MYB, bHLH, C2H2, and HSF families. In Vernicia lanceolata, MYB, ERF, and NAC significantly contribute to abiotic stress resistance [31]. Under drought stress, JIA2 transcription factors demonstrated both downregulation and upregulation, with downregulated factors such as MYB, WRKY, and HSF being more numerous. Various transcriptional regulatory mechanisms are involved in drought stress signal transduction pathways and stress responses in oats. Different genes within the same family exhibit diverse expression patterns under drought stress, reflecting their role in positive or negative regulation of stress response. Previous studies have also noted that a single transcription factor can interact with one or more members of the same or different families, indicating the complexity of transcription factors in plant drought stress response[32,33].

 doi:10.20944/preprints202501.1406.v1

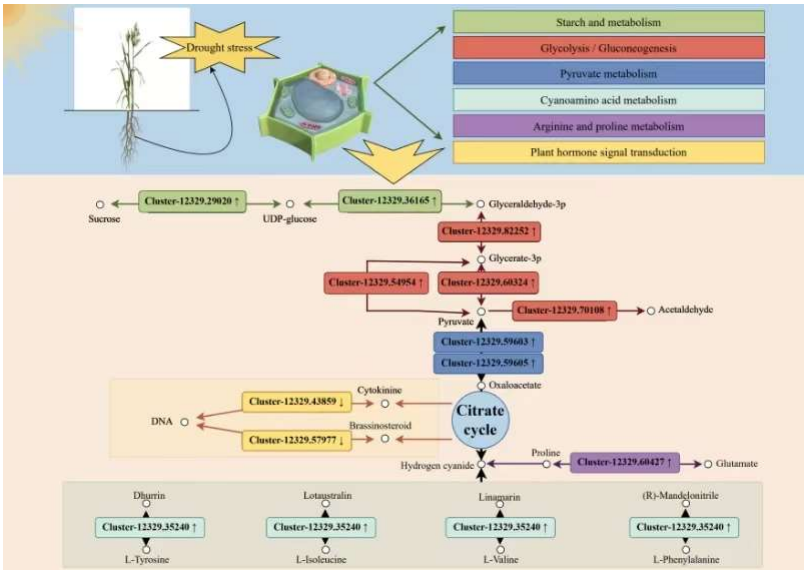

Figure 19. Schematic diagram of key metabolism response proteins and genes of drought tolerant cultivar JIA2 in response to drought stress (This figure is drawn by Figdraw).

4. Materials and Methods

4.1. Experimental Materials

The experiment utilized the drought-resistant cultivar JiaYan 2 (JIA2) and water-sensitive cultivar BaYou 9 (BA9), both preserved and bred in our laboratory.

4.2. Experimental Method

4.2.1. Oat Drought Stress Experiment

The experiment was conducted in a greenhouse at the Oat Industry Research Center of Inner Mongolia Agricultural University using potted plants. The soil for the pots was sandy loam with a field water-holding capacity of 16%. Oats were cultivated in plastic buckets measuring 25 cm in height, 24 cm in upper diameter, and 22 cm in lower diameter. Each bucket was filled with 10 kg (dry soil weight) of soil collected from the field tillage layer, and 3 g of diammonium phosphate and 3 g of urea were placed at the base. No topdressing was applied during the growth period. Before sowing, 1.5 L of water was added to moisten the bottom soil. Fifty seeds were sown per barrel, and 25 seedlings were maintained per barrel at the three-leaf stage. Two oat cultivars and three water stress gradients were set up, resulting in six treatments, with each treatment repeated eight times. Drought stress was applied during the jointing stage for a total of 48 barrels. The buckets were completely randomized, with their positions changed weekly. The three water gradients were 30% field capacity (severe stress), 45% field capacity (moderate stress), and 70% field capacity (normal water supply). Treatments were designated as BA9-1, 2, and 3, and JIA2-1, 2, and 3, representing normal water supply (70%), moderate drought stress (45%), and severe drought stress (30%) for BA9 and JIA2, respectively. Starting at the jointing stage (40 days after emergence), a 7-day water control treatment was applied daily using the weight difference method once each treatment reached the set water gradient. The oat root system, after treatment, served as the research focus for transcriptomics and proteomics analyses.

 doi:10.20944/preprints202501.1406.v1

4.2.2. Transcriptome Sequencing Analysis of Oat Root

Extraction and Qualification of RNA

Total RNA was extracted from the samples using TRIzol (Invitrogen, Carlsbad CA, USA). Complimentary DNA was synthesized from the RNA using the Reverse Transcriptase M-MLV Kit (TaKaRa). The RNA was analyzed using a NanoPhotometer® spectrophotometer (IMPLEN, CA, USA) and resolved on 1% agarose gels to verify shearing and quality. Library preparation and deep sequencing were conducted at Novogene Bioinformatics Technology Co. Ltd. (Beijing, China).

Transcriptome Sequencing and Quality Control

We used 1.5 μg of RNA per sample in the RNA sample preparation process. The NEBNext® Ultra™ RNA Library Prep Kit for Illumina® (NEB, USA) was used to prepare sequencing libraries. Sequencing was performed on an Illumina Hiseq platform. Raw sequencing data were filtered using an integrated approach: Trimmed for reads with N constitutes, adapter contamination, and low-quality reads with 50% of bases having Qphred ≤ 20.

Gene Annotation, Different Expression, and Enrichment Analyses

We assembled the trimmed reads using Trinity (version 2.5.1). The number of reads mapped to the reference genome was calculated using RSEM. Gene expression levels were estimated based on gene length and the number of reads expressed as fragments per kilobase of exon per million mapped reads (FPKM). Parallelism among replicate groups was assessed using Pearson correlation analysis. We conducted differentialDifferential gene expression analysis between the two conditions/groups was conducted using the DESeq2 package. P-values were adjusted using Benjamini and Hochberg's approach to control the false discovery rate. Genes with an adjusted P-value < 0.05, as determined by DESeq2, were considered differentially expressed. Kyoto encyclopedia of genes and genomes (KEGG) and gene ontology (GO) analyses were subsequently performed to predict the pathways and functions of the DEGs.

qRT-PCR Analysis

All qRT-PCR experiments were conducted in triplicate using a LightCycler 480 instrument (Roche Applied Science, Mannheim, Germany). Primers targeting choriolysin genes were used, with actin serving as the housekeeping gene (primer sequences are listed in Table 7). Choriolysin mRNA levels were calculated using the $2^{-\Delta\Delta Ct}$ method, and results are presented as mean ± standard error of the mean. Statistical analysis was performed using one-way ANOVA.

4.2.3. Application of Label-Free Technology for Oat Root Proteome Sequencing

Extraction of Total Protein from Oat Roots

The frozen samples were crushed using a liquid nitrogen-precooled crusher and ground further with liquid nitrogen. The resulting powder was mixed with lysis buffer at a 1:10 (w/v) ratio and vortexed. Ultrasonication was performed for 60 s, alternating 0.2 s on and 2 s off at 22% amplitude. Proteins were extracted at room temperature for 30 min, followed by centrifugation at 15,000 × g for 1 h at 10 ℃. The supernatant was collected, divided, and stored at −80 ℃.

Protein Quantification

Protein concentrations were determined using the Bradford method. The concentrations (μg μL−1) were calculated based on the curve formula. For detailed procedural steps, please refer to the study.

 doi:10.20944/preprints202501.1406.v1

Proteolysis (Filter-Aided Sample Preparation)

After protein quantification, 200 μg protein solution was transferred to a centrifuge tube, and DTT was added to make a final concentration of 25 mmol L–1. The solution was then reacted at 60 ℃ for 1 h, followed by the addition of iodoacetamide to make a final concentration of 50 mmol L–1. The solution was maintained at room temperature for 10 min. After reductive alkylation, the protein solution was transferred to a 10 K ultrafiltration tube and centrifuged at 12,000 × g for 20 min. The filtrate was collected, and 100 μL dissolution buffer was added. This step was repeated three times, and the filtrate was discarded after each centrifugation. Trypsin was then added to a new ultrafiltration tube, making a solution with a total protein mass of 4 μg (trypsin-to-protein ratio of 1:50) and volume of 50 μL. The reaction was incubated overnight at 37 ℃. The following day, the solution was centrifuged at 12,000 × g for 20 min, and the peptide solution in the filtrate was collected after enzymatic digestion. An additional 50 μL dissolution buffer was added to the ultrafiltration tube, followed by centrifugation at 12,000 × g for 20 min. The resulting solution was combined with the previously collected peptide solution, yielding a total volume of 100 μL in the collection tube after enzymolysis. Finally, the solution was lyophilized in preparation for loading.

Nano-Upgraded Reversed-Phase Chromatography-Q Exactive for Protein Analysis

A solution of 20 μL containing 2% methanol and 0.1% formic acid was prepared for this experiment. The solution was centrifuged at 12,000 × g for 10 min, and the supernatant was collected for sample loading. A sample volume of 10 μL was loaded using a loading pump with a flow rate of 350 nL min^{-1} for 15 min, while the separation flow rate was 300 nL min^{-1}.

Mass Spectrometry Data Analysis

The UniProt-Pooideae361804_20170619.fasta database (362,934 sequences) was used for analysis. Mass spectrometry analysis was performed with a Thermo Q Exactive mass spectrometer. Peptide Spectrum Matches with reliability exceeding 95% were considered trusted, while proteins containing at least one unique peptide were designated as trusted proteins. This study included only trusted peptides and proteins, with FDR verification applied to exclude peptides with FDR greater than 1% and egg whites. Proteins differing between paired samples across replicate groups were analyzed, and the mean value of the different multiples was used to quantify differences between samples. A t-test was conducted to calculate the P-value, which was used as the significance index.

Data Processing and Bioinformatics Analysis

Microsoft Excel 2010 and Statistical Analysis System (version 9.0) software were used for statistical analysis. Common functional database annotations for the identified proteins were conducted using COG, GO, and KEGG databases. Differential protein functional analyses, including GO and KEGG enrichment analyses, were performed for the selected differentially expressed proteins (DEPs).

5. Conclusions

Transcriptomic analysis revealed that under drought stress, JIA2 exhibited a higher number of DEGs compared with BA9. Most DEGs in JIA2 were downregulated, primarily associated with redox reactions, carbohydrate metabolism, plant growth hormone signaling regulation, and secondary metabolism. Proteomic analysis indicated significant differences in the number of upregulated and downregulated DEPs between the two cultivars under severe drought stress. A total of 314 specific DEPs were identified in JIA2, with an approximately equal number of upregulated and downregulated proteins. These proteins were predominantly involved in functions such as structural constant of the ribosome, protein binding, oxidation-reduction process, an integral component of membrane, catalytic activity, metabolic process, and carbohydrate metabolic process. The KEGG functional enrichment analysis of cor DEGs-DEPs indicated that under moderate stress, most DEGs

 doi:10.20944/preprints202501.1406.v1

and proteins in BA9 were upregulated, while some were downregulated, with a few exhibiting opposing expression trends. These are mainly related to metabolic pathways, secondary metabolites biosynthesis, and pathways for arginine and proline metabolism. Under severe stress, BA9 demonstrated a roughly equal number of upregulated and downregulated DEGs and DEPs, with the total number being relatively small. These were primarily associated with metabolic pathways and plant signal transduction pathways. Under moderate stress, JIA2 upregulated cor DEGs-DEPs, primarily involving metabolic pathways, biosynthesis of secondary metabolites, and ribosome biogenesis in eukaryotes. Downregulation of cor DEGs and DEPs mainly involved metabolic pathways such as glutathione metabolism, plant-pathogen interactions, linoleic acid metabolism, nitrogen metabolism, and phagocytosis. Under severe stress, JIA2 upregulated cor DEGs and DEPs, mainly involving metabolic pathways, starch and sucrose metabolism, biosynthesis of secondary metabolites, linoleic acid metabolism, pyruvate metabolism, and amino sugar and nucleotide sugar metabolism pathways. Downregulation of cor DEGs and DEPs primarily involved metabolic pathways such as starch and sucrose metabolism, biosynthesis of secondary metabolites, phagosomes, plant hormone signal transduction, and nitrogen metabolism. Under severe stress, JIA2 identified four types of DEPs that interacted with each other in differential gene-protein interaction network analysis. These proteins are mainly involved in plant hormone signal transduction, biosynthesis of secondary metabolites, carbohydrate metabolism processes, and metabolic pathways, including 13 key cor DEGs and DEPs. Future research should focus on further exploring DEGs and molecular markers related to these pathways, contributing to the breeding of drought-resistant oat cultivars.

Author Contributions: Conceptualization, X.C. and Z.X.; methodology, X.C; software, J.M.; validation, X.C., J.L. and B.Z.; formal analysis, B.Z.; investigation, Z.X.; resources, J.L.; data curation, X.C.; writing—original draft preparation, X.C.; writing—review and editing, Z.X.; visualization, J.L.; supervision, B.Z.; project administration, J.M.; funding acquisition, Z.X. All authors have read and agreed to the published version of the manuscript.

Funding: This research was funded by Inner Mongolia Agricultural University Project (NDYB2022-8) and National Modern Agricultural Industry Technology System(CARS-08-B-5).

Data Availability Statement: Proteomic and transcriptomic data will be provided during review. They must be provided prior to publication.

Acknowledgments: Our sample testing data analysis were assisted by Beijing Novogene Technology Co., Ltd. (Beijing, China).

Conflicts of Interest: The authors declare no conflicts of interest.

References

1. Bakhoum, G.S.; Sadak, M.S.; Thabet, M.S. Induction of Tolerance in Groundnut Plants against Drought Stress and Cercospora Leaf Spot Disease with Exogenous Application of Arginine and Sodium Nitroprusside under Field Conditions. J. Soil Sci. Plant Nutr. 2023, 23, 6612–6631.
2. Fathi, A.; Tari, D.B. Effect of Drought Stress and Its Mechanism in Plants. 2016.
3. Zandalinas, S.I.; Mittler, R.; Balfagón, D.; Arbona, V.; Gómez-Cadenas, A. Plant Adaptations to the Combination of Drought and High Temperatures. Physiol. Plant. 2018, 162, 2–12.
4. Guo, Y.-Y.; Yu, H.-Y.; Kong, D.-S.; Yan, F.; Zhang, Y.-J. Effects of Drought Stress on Growth and Chlorophyll Fluorescence of Lycium Ruthenicum Murr. Seedlings. Photosynthetica. 2016, 54, 524–531.
5. Maatallah, S.; Nasri, N.; Hajlaoui, H.; Albouchi, A.; Elaissi, A. Evaluation Changing of Essential Oil of Laurel (Laurus Nobilis L.) under Water Deficit Stress Conditions. Ind. Crops Prod. 2016, 91, 170–178.
6. Okunlola, G.O.; Olatunji, O.A.; Akinwale, R.O.; Tariq, A.; Adelusi, A.A. Physiological Response of the Three Most Cultivated Pepper Species (Capsicum Spp.) in Africa to Drought Stress Imposed at Three Stages of Growth and Development. Sci. Hortic. (Amsterdam). 2017, 224, 198–205.

7. Fang, Y.; Xiong, L. General Mechanisms of Drought Response and Their Application in Drought Resistance Improvement in Plants. Cell. Mol. life Sci. 2015, 72, 673–689.
8. Khan, M.S.; Ahmad, D.; Khan, M.A. Utilization of Genes Encoding Osmoprotectants in Transgenic Plants for Enhanced Abiotic Stress Tolerance. Electron. J. Biotechnol. 2015, 18, 257–266.
9. Ma, Q.; Shi, C.; Su, C.; Liu, Y. Complementary Analyses of the Transcriptome and ITRAQ Proteome Revealed Mechanism of Ethylene Dependent Salt Response in Bread Wheat (Triticum Aestivum L.). Food Chem. 2020, 325, 126866.
10. Michaletti, A.; Naghavi, M.R.; Toorchi, M.; Zolla, L.; Rinalducci, S. Metabolomics and Proteomics Reveal Drought-Stress Responses of Leaf Tissues from Spring-Wheat. Sci. Rep. 2018, 8, 5710.
11. Lv, L.; Zhao, A.; Zhang, Y.; Li, H.; Chen, X. Proteome and Transcriptome Analyses of Wheat near Isogenic Lines Identifies Key Proteins and Genes of Wheat Bread Quality. Sci. Rep. 2021, 11, 9978.
12. Shinozaki, K.; Yamaguchi-Shinozaki, K. Gene Networks Involved in Drought Stress Response and Tolerance. J. Exp. Bot. 2007, 58, 221–227.
13. Joshi, R.; Wani, S.H.; Singh, B.; Bohra, A.; Dar, Z.A.; Lone, A.A.; Pareek, A.; Singla-Pareek, S.L. Transcription Factors and Plants Response to Drought Stress: Current Understanding and Future Directions. Front. Plant Sci. 2016, 7, 1029.
14. Clemens, R.; van Klinken, B.J.-W. Oats, More than Just a Whole Grain: An Introduction. Br. J. Nutr. 2014, 112, S1–S3.
15. Ren, C.Z.; Hu, Y.G. Chinese Oatology. Beijing, China Agric. Press. Chinese) 2013, 1, 211–220.
16. Ghimire, K.; McIntyre, I.; Caffe, M. Evaluation of Morpho-Physiological Traits of Oat (Avena Sativa L.) under Drought Stress. Agriculture 2024, 14, 109.
17. Qiao, M.; Lv, S.; Qiao, Y.; Lin, W.; Gao, Z.; Tang, X.; Yang, Z.; Chen, J. Exogenous Streptomyces Spp. Enhance the Drought Resistance of Naked Oat (Avena Nuda) Seedlings by Augmenting Both the Osmoregulation Mechanisms and Antioxidant Capacities. Funct. Plant Biol. 2024, 51.
18. Zhang, X.; Liu, W.; Lv, Y.; Li, T.; Tang, J.; Yang, X.; Bai, J.; Jin, X.; Zhou, H. Effects of Drought Stress during Critical Periods on the Photosynthetic Characteristics and Production Performance of Naked Oat (Avena Nuda L.). Sci. Rep. 2022, 12, 11199.
19. Gong, W.; Ju, Z.; Chai, J.; Zhou, X.; Lin, D.; Su, W.; Zhao, G. Physiological and Transcription Analyses Reveal the Regulatory Mechanism in Oat (Avena Sativa) Seedlings with Different Drought Resistance under PEG-Induced Drought Stress. Agronomy 2022, 12, 1005.
20. Wang, Y.; Lysøe, E.; Armarego-Marriott, T.; Erban, A.; Paruch, L.; Van Eerde, A.; Bock, R.; Liu-Clarke, J. Transcriptome and Metabolome Analyses Provide Insights into Root and Root-Released Organic Anion Responses to Phosphorus Deficiency in Oat. J. Exp. Bot. 2018, 69, 3759–3771.
21. Lou, X.; Wang, H.; Ni, X.; Gao, Z.; Iqbal, S. Integrating Proteomic and Transcriptomic Analyses of Loquat (Eriobotrya Japonica Lindl.) in Response to Cold Stress. Gene 2018, 677, 57–65.
22. Oshone, R.; Ngom, M.; Chu, F.; Mansour, S.; Sy, M.O.; Champion, A.; Tisa, L.S. Genomic, Transcriptomic, and Proteomic Approaches towards Understanding the Molecular Mechanisms of Salt Tolerance in Frankia Strains Isolated from Casuarina Trees. BMC Genomics 2017, 18, 1–21.
23. Chen, J.; Song, Y.; Zhang, H.; Zhang, D. Genome-Wide Analysis of Gene Expression in Response to Drought Stress in Populus Simonii. Plant Mol. Biol. Report. 2013, 31, 946–962.
24. Liu, S.-C.; Jin, J.-Q.; Ma, J.-Q.; Yao, M.-Z.; Ma, C.-L.; Li, C.-F.; Ding, Z.-T.; Chen, L. Transcriptomic Analysis of Tea Plant Responding to Drought Stress and Recovery. PLoS One 2016, 11, e0147306.
25. Wang, W.; Xin, H.; Wang, M.; Ma, Q.; Wang, L.; Kaleri, N.A.; Wang, Y.; Li, X. Transcriptomic Analysis Reveals the Molecular Mechanisms of Drought-Stress-Induced Decreases in Camellia Sinensis Leaf Quality. Front. Plant Sci. 2016, 7, 385.
26. Alvarez, S.; Roy Choudhury, S.; Pandey, S. Comparative Quantitative Proteomics Analysis of the ABA Response of Roots of Drought-Sensitive and Drought-Tolerant Wheat cultivars Identifies Proteomic Signatures of Drought Adaptability. J. Proteome Res. 2014, 13, 1688–1701.
27. Bai, J.; Liu, J.; Jiao, W.; Sa, R.; Zhang, N.; Jia, R. Proteomic Analysis of Salt-responsive Proteins in Oat Roots (Avena Sativa L.). J. Sci. Food Agric. 2016, 96, 3867–3875.

 doi:10.20944/preprints202501.1406.v1

28. Schachtman, D.P.; Goodger, J.Q.D. Chemical Root to Shoot Signaling under Drought. Trends Plant Sci. 2008, 13, 281–287.
29. Ramadan, A.; Sabir, J.S.M.; Alakilli, S.Y.M.; Shokry, A.M.; Gadalla, N.O.; Edris, S.; Al-Kordy, M.A.; Al-Zahrani, H.S.; El-Domyati, F.M.; Bahieldin, A. Metabolomic Response of Calotropis Procera Growing in the Desert to Changes in Water Availability. PLoS One 2014, 9, e87895.
30. Wang, H.; Wang, H.; Shao, H.; Tang, X. Recent Advances in Utilizing Transcription Factors to Improve Plant Abiotic Stress Tolerance by Transgenic Technology. Front. Plant Sci. 2016, 7, 67.
31. Wang, B.; Lv, X.-Q.; He, L.; Zhao, Q.; Xu, M.-S.; Zhang, L.; Jia, Y.; Zhang, F.; Liu, F.-L.; Liu, Q.-L. Whole-Transcriptome Sequence Analysis of Verbena Bonariensis in Response to Drought Stress. Int. J. Mol. Sci. 2018, 19, 1751.
32. Dastmalchi, M.; Chapman, P.; Yu, J.; Austin, R.S.; Dhaubhadel, S. Transcriptomic Evidence for the Control of Soybean Root Isoflavonoid Content by Regulation of Overlapping Phenylpropanoid Pathways. BMC Genomics 2017, 18, 1–15.
33. Ye, G.; Ma, Y.; Feng, Z.; Zhang, X. Transcriptomic Analysis of Drought Stress Responses of Sea Buckthorn (Hippophae Rhamnoides Subsp. Sinensis) by RNA-Seq. PLoS One 2018, 13, e0202213.